LAWRENCE
LIVERMORE
NATIONAL
LABORATORY

LLNL-JRNL-420356

Asymptotic Diffusion-Limit Accuracy of Sn Angular Differencing Schemes

Teresa S. Bailey, Jim E. Morel, Jae H. Chang

November 17, 2009

Nuclear Science and Engineering

Disclaimer

Asymptotic Diffusion-Limit Accuracy of S_n Angular Differencing Schemes

Teresa S. Bailey

Lawrence Livermore National Laboratory
P.O. Box 808, L-095
Livermore, CA 94551

bailey42@llnl.gov

Jim E. Morel

Texas A&M University
Department of Nuclear Engineering
129 Zachry Engineering Center, TAMU3133
College Station, Texas 77843-3133

morel@tamu.edu

Jae H. Chang

Los Alamos National Laboratory
P.O. Box 1663, MS D409
Los Alamos, NM 87544

jhchang@lanl.gov

Pages: 55
Tables: 2
Figures: 12

Send proofs and page charges to:

Teresa Bailey
Lawrence Livermore National Laboratory
P.O. Box 808, L-095
Livermore, CA 94551
(925) 424-6700
bailey42@llnl.gov

Asymptotic Diffusion-Limit Accuracy of S_n Angular Differencing Schemes

Teresa S. Bailey
Lawrence Livermore National Laboratory
P.O. Box 808, L-095
Livermore, CA 94551

Jim E. Morel
Texas A&M University
Department of Nuclear Engineering
129 Zachry Engineering Center, TAMU3133
College Station, Texas 77843-3133

Jae H. Chang
Los Alamos National Laboratory
P.O. Box 1663, MS D409
Los Alamos, NM 87544

Abstract

In a previous paper, Morel and Montry used a Galerkin-based diffusion analysis to define a particular weighted diamond angular discretization for S_n calculations in curvilinear geometries. The weighting factors were chosen to ensure that the Galerkin diffusion approximation was preserved, which eliminated the discrete-ordinates flux dip. It was also shown that the step and diamond angular differencing schemes, which both suffer from the flux dip, do not preserve the diffusion approximation in the Galerkin sense. In this paper we re-derive the Morel and Montry weighted diamond scheme using a formal asymptotic diffusion-limit analysis. The asymptotic analysis yields more information than the Galerkin analysis and demonstrates that the step and diamond schemes do in fact formally preserve the diffusion limit to leading order, while the Morel and Montry weighted diamond scheme preserves it to first order, which is required for full consistency in this limit. Nonetheless, the fact that the step and diamond differencing schemes preserve the diffusion limit to leading order suggests that the flux dip should disappear as the diffusion limit is approached for these schemes. Computational results are presented that confirm this conjecture. We further conjecture that preserving the Galerkin diffusion approximation is equivalent to preserving the asymptotic diffusion limit to first order.

1. Introduction

It is well known that the diffusion equation can be derived from the transport equation through a Galerkin approximation based upon an angular trial space that is linear in the direction cosines.[1] Morel and Montry[2] used a Galerkin-based diffusion analysis to define a particular weighted diamond angular discretization scheme for S_n calculations in curvilinear geometries. The Morel and Montry weighted diamond weighting factors were chosen to ensure that the diffusion approximation was preserved, and preservation of this approximation was found to eliminate the discrete-ordinates flux dip. It was also shown that the step and diamond angular differencing schemes, which were known to suffer from the flux dip, do not preserve the Galerkin diffusion approximation. In this paper we revisit the derivation of the weighted diamond scheme using a formal asymptotic diffusion-limit analysis[3,4] rather than one based upon a Galerkin diffusion approximation. The asymptotic analysis yields more information than the Galerkin analysis, and demonstrates that the step and diamond schemes do in fact formally preserve the diffusion limit to leading order, whereas the weighted diamond scheme preserves it to first order. Full consistency in the diffusion limit requires first-order asymptotic preservation because the diffusion approximation itself is correct to first order. If a numerical method does not preserve the diffusion limit through first order we conclude that it is not as accurate as a method which does preserve the diffusion limit through first order; methods that preserve the diffusion limit through leading order only do not represent the physics as well as methods which preserve the diffusion limit through first order. Nonetheless, the fact that the step and diamond differencing schemes

preserve the diffusion limit to leading order suggests that when these schemes are used, the flux dip should disappear as the diffusion limit is approached. Computational results are presented that confirm this conjecture. In this paper, when we refer to the accuracy of a method, we refer to the extent to which it preserves the diffusion limit, i.e., its asymptotic order of accuracy in that limit. With this definition, a method that preserves the diffusion limit to first order is more accurate, or consistent with the analytic diffusion limit, than a scheme that only preserves it to leading order. Our discussion of the computational results reflects this definition. While it might appear that the original Galerkin analysis is in contradiction to the asymptotic analysis, we believe that this is actually not the case. Rather we conjecture that preservation of the Galerkin diffusion approximation is equivalent to preservation of the asymptotic diffusion limit to first order.

The remainder of this paper is organized as follows. In Section 2, we discuss the Galerkin approach for defining preservation of the diffusion limit. In Section 3, we discuss the asymptotic approach. In Section 4, we apply the asymptotic analysis to the S_n equations in 1D spherical geometry with general weighted diamond differencing. We show that while the diffusion limit is preserved to leading order independent of the auxiliary weighted diamond relationship, only the weighted diamond relationship of Morel and Montry preserves the asymptotic diffusion limit to first order. In Section 5 we apply the asymptotic diffusion-limit analysis to the S_n equations with general weighted diamond angular differencing in RZ geometry and show results analogous to those obtained in 1D spherical geometry. In Section 6 we present computational results demonstrating that the flux dip does not appear with the weighted diamond scheme of

Morel and Montry in both 1D spherical and 2D cylindrical geometries. We also present results in both 1D spherical geometry and 2D cylindrical geometry demonstrating that the diamond scheme satisfies the diffusion limit to leading order and that the flux dip disappears in this limit. Finally in Sections 7 and 8 we argue that the Galerkin and asymptotic analyses are not contradictory, and suggest research for the future.

2. The Galerkin-Based Diffusion Analysis

Morel and Montry defined the following technique for determining if an S_n scheme preserves the Galerkin diffusion approximation in 1-D spherical geometry.

1. Begin with the 1-D spherical-geometry S_n equations discretized only in angle.
2. Assume a discrete angular flux solution of the following linear form:

$$\psi_m = \frac{1}{4\pi}\phi + \frac{3}{4\pi} J_r \mu_m \quad , \tag{1}$$

   where ψ_m is the angular flux in direction m, ϕ is the scalar flux, and J_r *is* the radial component of the current.
3. Numerically integrate the S_n equations over all directions to obtain the balance equation. All standard S_n discretizations ensure that a balance equation is obtained. This is the zeroth angular moment of the transport equation.
4. Multiply the S_n equations by μ_m and then numerically integrate to obtain an equation for the current. This is the first angular moment of the transport equation.

5. If the equation for the current is equivalent to Fick's law, then the S_n equations are said to preserve the Galerkin diffusion approximation because the current can be eliminated from the balance equation to obtain the diffusion equation.

This technique is useful, but it only involves the end-state of the diffusion limit. It assumes that the angular flux has a linear dependence, but it does not define a physical process that drives the transport solution to that state. This approach gives no information about when or why the angular flux should assume a linear dependence. We simply know that if we assume a linear dependence, the analytic transport solution will satisfy the diffusion equation. In the next section we show that an asymptotic diffusion limit analysis is much more useful than the Galerkin diffusion analysis. The asymptotic approach defines a true limiting process in which the transport solution is driven to a diffusive dependence.

3. The Asymptotic Diffusion Limit Analysis

We can show that the transport equation limits to a diffusion equation by performing an asymptotic analysis on the properly scaled transport equation. In this analysis we first scale the physical parameters in the transport equation by a small parameter, ε, such that the problem becomes optically thick and diffusive in the limit as $\varepsilon \to 0$. As a result,

$$\begin{aligned} \sigma_t &\to \frac{\sigma_t}{\varepsilon} \\ \sigma_a &\to \varepsilon\sigma_a \\ Q &\to \varepsilon Q \quad . \end{aligned} \tag{2}$$

We then expand the angular flux solution in terms of a power series of ε,

$$\psi_m(r) = \psi_m^{(0)} + \varepsilon\psi_m^{(1)} + \varepsilon^2\psi_m^{(2)}\ldots, \tag{3}$$

and substitute this expression into the transport equation. This results in a hierarchy of equations with each equation corresponding to the coefficients of a given power of ε. We solve these equations to determine how our scaled equation behaves in the diffusion limit. Larsen and Keller[3] have shown that when this analysis is performed on the analytic transport equation with isotropic scattering and an isotropic distributed source, the leading-order angular flux is isotropic:

$$\psi^{(0)} = \frac{1}{4\pi}\phi^{(0)} \quad , \tag{4}$$

and the leading-order scalar flux satisfies the following diffusion equation in the interior of a thick, diffusive problem

$$-\vec{\nabla}\cdot D\vec{\nabla}\phi^{(0)} + \sigma_a\phi^{(0)} = Q \quad . \tag{5}$$

Furthermore, the first-order scalar flux similarly satisfies a diffusion equation:

$$-\vec{\nabla}\cdot D\vec{\nabla}\phi^{(1)} + \sigma_a\phi^{(1)} = 0 \quad . \tag{6}$$

Multiplying Eq.(6) by ε and adding it to Eq.(5), we see that the scalar flux through first order satisfies the same diffusion equation as the leading-order scalar flux:

$$-\vec{\nabla}\cdot D\vec{\nabla}(\phi^{(0)} + \varepsilon\phi^{(1)}) + \sigma_a(\phi^{(0)} + \varepsilon\phi^{(1)}) = Q \quad . \tag{7}$$

Further analysis shows that the diffusion approximation has a second-order asymptotic error in the diffusion limit:

$$-\vec{\nabla}\cdot D\vec{\nabla}\phi + \sigma_a \phi = Q + O(\varepsilon^2) \ . \qquad (8)$$

Larsen, Morel, and Miller[4] have shown that if a discretized form of the transport equation limits to an accurate discretized diffusion equation for the leading-order scalar flux under the same scaling, the discretization will produce accurate results in highly diffusive problems. However, to achieve completely consistent behavior with the diffusion limit, it is necessary to obtain an accurate diffusion discretization for the first-order scalar flux as well. This higher level of accuracy, as indicated by higher order preservation of the diffusion limit, has generally been neglected in developing S_n spatial discretization schemes, but we show here that retaining full first-order consistency can be important for angular discretizations. In particular, we perform the asymptotic analysis for a variety of angular discretizations in 1D spherical and 2D cylindrical geometry. Each discretization we analyze produces good results for the leading-order scalar flux, but only the weighted diamond difference discretization developed by Morel and Montry produces a good diffusion approximation for the first-order scalar flux in the asymptotic diffusion limit. Computational testing indicates that preserving first-order consistency in the diffusion limit eliminates the flux dip in general, while preserving leading-order consistency in the diffusion limit only eliminates the flux dip in highly diffusive problems.

It is interesting to note that, unlike the Galerkin-based analysis, the asymptotic analysis requires no assumptions about the angular shape of the solution. One need only

assume a physical scaling of the transport equation that drives the transport solution to a diffusion limit as the scaling parameter approaches zero.

4. The Asymptotic Analysis for 1D spherical geometry

The one-dimensional spherical-geometry transport equation with isotropic scattering and an isotropic distributed source is given in conservation form[1] by

$$\frac{\mu}{r^2}\frac{\partial}{\partial r}r^2\psi\left(r,\mu\right)+\frac{1}{r}\frac{\partial}{\partial\mu}\left(1-\mu^2\right)\psi\left(r,\mu\right)+\sigma_t\psi\left(r,\mu\right)=\frac{\sigma_s}{2}\phi+\frac{1}{2}Q\ . \tag{9}$$

When any standard S_n angular discretization is applied to Eq.(9), the result is

$$\begin{aligned}\mu_m\frac{\partial}{\partial r}r^2\psi_m\left(r\right)+r\frac{\alpha_{m+\frac{1}{2}}\psi_{m+\frac{1}{2}}\left(r\right)-\alpha_{m-\frac{1}{2}}\psi_{m-\frac{1}{2}}\left(r\right)}{w_m}+r^2\sigma_t\psi_m\left(r\right)\\ =\frac{r^2}{2}\sigma_s\phi\left(r\right)+\frac{r^2}{2}Q\ ,\end{aligned} \tag{10}$$

where the α–coefficients are obtained through a recursion relationship

$$\begin{aligned}\alpha_{m+\frac{1}{2}}=\alpha_{m-\frac{1}{2}}-2\mu_m w_m\ \ ,\\ \alpha_{\frac{1}{2}}=\alpha_{M+\frac{1}{2}}=0\ ,\\ \text{and}\\ \sum_{m=1}^{M}w_m=2\ .\end{aligned} \tag{11}$$

While $\alpha_{1/2}$ is set to zero to start the recursion, $\alpha_{M+1/2}$ will always be zero when computed recursively. The cell-edge cosines associated with Eq. (10) are also obtained via recursion

$$\begin{aligned}\mu_{m+\frac{1}{2}}=\mu_{m-\frac{1}{2}}+w_m\ \ ,\\ \mu_{\frac{1}{2}}=-1\ ,\ \mu_{M+\frac{1}{2}}=+1\ .\end{aligned} \tag{12}$$

While $\mu_{1/2}$ is explicitly set to -1 to start the recursion, $\mu_{M+1/2}$ will always be equal to +1 when computed recursively. We define the scalar flux and current as

$$\phi(r) = \sum_{m=1}^{M} w_m \psi_m(r) \tag{13}$$

and

$$J(r) = \sum_{m=1}^{M} w_m \mu_m \psi_m(r) \ , \tag{14}$$

respectively. The discretization as defined is not complete. To close the system, we must relate the cell-center and cell-edge fluxes. To do this generally, we assume a weighted diamond relationship between the cell-edge and cell-center cosines:

$$\psi_m = \tau_m \psi_{m+\frac{1}{2}} + (1-\tau_m)\psi_{m-\frac{1}{2}} \ , \tag{15}$$

where each weighting factor, τ_m, can take on any value between zero and one. Note that τ_m=1 gives the step scheme, and τ_m=1/2 gives the diamond scheme. Solving Eq. (15) for $\psi_{m+1/2}$, we get

$$\psi_{m+\frac{1}{2}} = \frac{1}{\tau_m}\psi_m - \frac{(1-\tau_m)}{\tau_m}\psi_{m-\frac{1}{2}} \ . \tag{16}$$

Equation (16) is a recursion that needs a starting flux, $\psi_{1/2}$. From Eq. (12), we find that the cosine corresponding to the starting value is $\mu_{1/2}=-1$. It is easily shown that the flux along this direction satisfies the following slab equation

$$-\frac{\partial}{\partial r}\psi_{\frac{1}{2}}(r) + \sigma_t \psi_{\frac{1}{2}}(r) = \frac{1}{2}\sigma_s \phi(r) + \frac{1}{2}Q \ . \tag{17}$$

The discretization is now complete, although the weighting factors are largely arbitrary. Finally we assume a standard S_n quadrature set that is symmetric about μ=0 and that

exactly integrates polynomials in μ through degree 2 (quadratic). Some useful properties of standard 1D quadrature sets are

$$\begin{aligned}\sum_{m=1}^{M} w_m \mu_m &= 0 \\ \sum_{m=1}^{M} w_m \mu_m^2 &= \frac{2}{3} \\ \sum_{m=1}^{M} w_m \mu_m^3 &= 0 \quad .\end{aligned} \tag{18}$$

To begin the asymptotic diffusion limit analysis, we substitute the scaled parameters in Eq. (2) into Eqs. (10) and (17), resulting in

$$\begin{aligned}\mu_m \frac{\partial}{\partial r} r^2 \psi_m(r) + r \frac{\alpha_{m+\frac{1}{2}} \psi_{m+\frac{1}{2}}(r) - \alpha_{m-\frac{1}{2}} \psi_{m-\frac{1}{2}}(r)}{w_m} + r^2 \frac{\sigma_t}{\varepsilon} \psi_m(r) \\ = \frac{r^2}{2}\left(\frac{\sigma_t}{\varepsilon} - \varepsilon\sigma_a\right)\phi(r) + \frac{r^2}{2}\varepsilon Q\end{aligned} \tag{19}$$

and

$$-\frac{\partial}{\partial r}\psi_{\frac{1}{2}}(r) + \frac{\sigma_t}{\varepsilon}\psi_{\frac{1}{2}}(r) = \frac{1}{2}\left(\frac{\sigma_t}{\varepsilon} - \varepsilon\sigma_a\right)\phi(r) + \frac{1}{2}\varepsilon Q \ , \tag{20}$$

where we note that $\sigma_s = \sigma_t - \sigma_a$. We then substitute our flux guesses from Eq. (3) into Eqs. (19) and (20), resulting in

$$
\begin{aligned}
&\mu_m \frac{\partial}{\partial r} r^2 \left[\psi_m^{(0)} + \varepsilon \psi_m^{(1)} + \varepsilon^2 \psi_m^{(2)} \ldots \right] \\
&+ r \frac{\alpha_{m+\frac{1}{2}}}{w_m} \left[\psi_{m+\frac{1}{2}}^{(0)} + \varepsilon \psi_{m+\frac{1}{2}}^{(1)} + \varepsilon^2 \psi_{m+\frac{1}{2}}^{(2)} \ldots \right] - \\
&r \frac{\alpha_{m-\frac{1}{2}}}{w_m} \left[\psi_{m-\frac{1}{2}}^{(0)} + \varepsilon \psi_{m-\frac{1}{2}}^{(1)} + \varepsilon^2 \psi_{m-\frac{1}{2}}^{(2)} \ldots \right] \\
&+ r^2 \frac{\sigma_t}{\varepsilon} \left[\psi_m^{(0)} + \varepsilon \psi_m^{(1)} + \varepsilon^2 \psi_m^{(2)} \ldots \right] = \\
&\frac{r^2}{2} \left(\frac{\sigma_t}{\varepsilon} - \varepsilon \quad _a \right) \left[\quad ^{(0)} \phi + \quad \varepsilon^{(1)} + \phi^2 \quad ^{(2)} \varepsilon \ldots \right] \phi \frac{r^2}{2} \varepsilon Q
\end{aligned}
\tag{21}
$$

and

$$
\begin{aligned}
&-\frac{\partial}{\partial r} \left[\psi_{\frac{1}{2}}^{(0)} + \varepsilon \psi_{\frac{1}{2}}^{(1)} + \varepsilon^2 \psi_{\frac{1}{2}}^{(2)} . \right] + \frac{\sigma_t}{\varepsilon} \left[\psi_{\frac{1}{2}}^{(0)} . + \varepsilon \psi_{\frac{1}{2}}^{(1)} + \varepsilon^2 \psi_{\frac{1}{2}}^{(2)} . \right] \\
&= \frac{1}{2} \left(\frac{\sigma_t}{\varepsilon} - \varepsilon \sigma_a \right) \left[\phi^{(0)} + \varepsilon \phi^{(1)} + \varepsilon^2 \phi^{(2)} \ldots \right] + \frac{1}{2} \varepsilon Q \ .
\end{aligned}
\tag{22}
$$

To proceed with the analysis we collect and equate the like order terms in Eqs. (21) and (22) to produce equations that describe the individual modes of the angular and scalar flux. From the *O(1/ε)* terms we find that the leading order cell-centered angular fluxes are:

$$
\psi_m^{(0)} = \frac{1}{2} \phi^{(0)} \ . \tag{23}
$$

and

$$
\psi_{\frac{1}{2}}^{(0)} = \frac{1}{2} \phi^{(0)} \ , \tag{24}
$$

for the spherical and starting direction equations, respectively. We can substitute Eqs. (23) and (24) into Eq. (16) and find that the cell-edge fluxes are also:

$$
\psi_{m+\frac{1}{2}}^{(0)} = \frac{1}{2} \phi^{(0)} \ . \tag{25}
$$

Equations (23), (24), and (25) imply that the leading-order angular flux is isotropic, which is in agreement with Eq. (4).

After some manipulation, the *O(1)* terms in Eq. (21), result in

$$\mu_m \frac{\partial}{\partial r}\frac{\phi^{(0)}}{2} + \sigma_t \psi_m{}^{(1)} = \frac{1}{2}\sigma_t \phi^{(1)} \quad . \tag{26}$$

In order to ensure a solvability condition, we take the zeroth angular moment of Eq. (26):

$$\frac{\partial}{\partial r}\frac{\phi^{(0)}}{2}\sum_{m=1}^{M} w_m \mu_m + \sigma_t \sum_{m=1}^{M} w_m \psi_m{}^{(1)} = \frac{1}{2}\sigma_t \phi^{(1)} \sum_{m=1}^{M} w_m \quad . \tag{27}$$

Using the definitions found in Eqs. (11), (13), and (18), Eq. (27) can be simplified to

$$\sigma_t \phi^{(1)} = \sigma_t \phi^{(1)} \quad , \tag{28}$$

which proves our solvability condition. We then find the first-order current by taking the first angular moment of Eq. (26), resulting in:

$$J^{(1)} = -\frac{1}{3\sigma_t}\frac{\partial}{\partial r}\phi^{(0)} \quad . \tag{29}$$

We now collect the *O(ε)* terms in Eq. (21), resulting in

$$\begin{aligned} \mu_m \frac{\partial}{\partial r} r^2 \psi_m{}^{(1)} + r\frac{\alpha_{m+\frac{1}{2}}\psi_{m+\frac{1}{2}}{}^{(1)} - \alpha_{m-\frac{1}{2}}\psi_{m-\frac{1}{2}}{}^{(1)}}{w_m} + r^2\sigma_t \psi_m{}^{(2)} \\ = \frac{r^2}{2}\sigma_t \phi^{(2)} - \frac{r^2}{2}\sigma_a \phi^{(0)} + \frac{r^2}{2} Q \quad . \end{aligned} \tag{30}$$

After applying the zeroth angular moment to Eq. (30), and performing some algebra Eq. (30) becomes

$$\frac{\partial}{\partial r} r^2 J^{(1)} + r^2 \sigma_a \phi^{(0)} = r^2 Q \quad . \tag{31}$$

Substituting Eq. (29) into Eq. (31) results in the following one-dimensional diffusion equation in spherical coordinates, which is in agreement with Eq.(5):

$$-\frac{\partial}{\partial r} r^2 \frac{1}{3\sigma_t} \frac{\partial}{\partial r} \phi^{(0)} + r^2 \sigma_a \phi^{(0)} = r^2 Q \ . \tag{32}$$

Thus, the leading-order flux is described by the correct diffusion equation with *any* choice of weighting factors in the approximation of the angular flux. As a result, we will not see an error in the flux at the origin for the step, diamond, and Morel and Montry weighted diamond discretizations when the system is sufficiently thick and diffusive such that the leading-order solution dominates higher-order components.

We now go a step further to determine the diffusion discretization for the first-order flux generated by the various angular differencing schemes. For the remainder of this analysis we will be explicit in describing the algebraic steps we use to arrive at our conclusions because the equation for the first-order flux is seldom derived for asymptotic analyses of the discretized transport equation. Collecting the $O(\varepsilon^2)$ terms in Eq. (21), we obtain

$$\mu_m \frac{\partial}{\partial r} r^2 \psi_m^{(2)} + r \frac{\alpha_{m+\frac{1}{2}} \psi_{m+\frac{1}{2}}^{(2)} - \alpha_{m-\frac{1}{2}} \psi_{m-\frac{1}{2}}^{(2)}}{w_m} + r^2 \sigma_t \psi_m^{(3)} = \frac{r^2}{2} \sigma_t \phi^{(3)} - \frac{r^2}{2} \sigma_a \phi^{(1)} \ . \tag{33}$$

We then take the zeroth moment of this equation. After some algebra, the equation simplifies to:

$$\frac{\partial}{\partial r} r^2 J^{(2)} + r^2 \sigma_a \phi^{(1)} = 0 \ . \tag{34}$$

If we can find a Fick's law relationship for $J^{(2)}$ in terms of $\phi^{(1)}$, then we will obtain the correct diffusion discretization for the first-order flux. First, we use Eq. (26) to solve for the first-order angular flux, $\psi_m^{(1)}$:

$$\psi_m^{(1)} = \frac{1}{2}\phi^{(1)} - \frac{\mu_m}{\sigma_t}\frac{\partial}{\partial r}\frac{\phi^{(0)}}{2} \quad . \tag{35}$$

We then substitute this relationship into Eq. (30):

$$\begin{aligned} &\mu_m \frac{\partial}{\partial r} r^2 \left(\frac{1}{2}\phi^{(1)} - \frac{\mu_m}{\sigma_t}\frac{\partial}{\partial r}\frac{\phi^{(0)}}{2} \right) \\ &+r\frac{\alpha_{m+\frac{1}{2}}\left[\frac{1}{2}\phi^{(1)} - \frac{\mu_{m+\frac{1}{2}}}{\sigma_t}\frac{\partial}{\partial r}\frac{\phi^{(0)}}{2} \right] - \alpha_{m-\frac{1}{2}}\left[\frac{1}{2}\phi^{(1)} - \frac{\mu_{m+\frac{1}{2}}}{\sigma_t}\frac{\partial}{\partial r}\frac{\phi^{(0)}}{2} \right]}{w_m} \\ &+r^2\sigma_t\psi_m^{(2)} = \frac{r^2}{2}\sigma_t\phi^{(2)} - \frac{r^2}{2}\sigma_a\phi^{(0)} + \frac{r^2}{2}Q \quad . \end{aligned} \tag{36}$$

In order to solve for $J^{(2)}$, we take the first angular moment of Eq. (36):

$$\begin{aligned} &\frac{\partial}{\partial r}\frac{r^2}{2}\phi^{(1)}\sum_{m=1}^{M} w_m\mu_m^2 - \frac{1}{\sigma_t}\frac{\partial}{\partial r} r^2 \frac{\partial}{\partial r}\frac{\phi^{(0)}}{2}\sum_{m=1}^{M} w_m\mu_m^3 \\ &+r\frac{1}{2}\phi^{(1)}\sum_{m=1}^{M}\mu_m\left[\alpha_{m+\frac{1}{2}} - \alpha_{m-\frac{1}{2}}\right] \\ &-r\frac{1}{\sigma_t}\frac{\partial}{\partial r}\frac{\phi^{(0)}}{2}\sum_{m=1}^{M}\mu_m\left[\alpha_{m+\frac{1}{2}}\mu_{m+\frac{1}{2}} - \alpha_{m-\frac{1}{2}}\mu_{m-\frac{1}{2}}\right] \\ &+r^2\sigma_t\sum_{m=1}^{M} w_m\mu_m\psi_m^{(2)} = \frac{r^2}{2}\sigma_t\phi^{(2)}\sum_{m=1}^{M} w_m\mu_m - \frac{r^2}{2}\sigma_a\phi^{(0)}\sum_{m=1}^{M} w_m\mu_m + \frac{r^2}{2}Q\sum_{m=1}^{M} w_m\mu_m \quad . \end{aligned} \tag{37}$$

The requirements of our quadrature set in Eq. (18) and the definition of α–coefficients in Eq. (11) cause Eq. (37) to simplify to

$$\begin{aligned} &\frac{\partial}{\partial r}\frac{r^2}{2}\phi^{(1)}\sum_{m=1}^{M} w_m\mu_m^2 - r\frac{\phi^{(1)}}{2}2\sum_{m=1}^{M} w_m\mu_m^2 \\ &-r\frac{1}{\sigma_t}\frac{\partial}{\partial r}\frac{\phi^{(0)}}{2}\sum_{m=1}^{M}\mu_m\left[\alpha_{m+\frac{1}{2}}\mu_{m+\frac{1}{2}} - \alpha_{m-\frac{1}{2}}\mu_{m-\frac{1}{2}}\right] + r^2\sigma_t J^{(2)} = 0 \quad . \end{aligned} \tag{38}$$

The first term in Eq. (38) can be expanded using the chain rule for differentiation, causing the equation to simplify to

$$\frac{r^2}{3}\frac{\partial}{\partial r}\phi^{(1)} - r\frac{1}{\sigma_t}\frac{\partial}{\partial r}\frac{\phi^{(0)}}{2}\sum_{m=1}^{M}\mu_m\left[\alpha_{m+\frac{1}{2}}\mu_{m+\frac{1}{2}} - \alpha_{m-\frac{1}{2}}\mu_{m-\frac{1}{2}}\right] + r^2\sigma_t J^{(2)} = 0 \ . \qquad (39)$$

Solving for the current results in

$$J^{(2)} = -\frac{1}{3\sigma_t}\frac{\partial}{\partial r}\phi^{(1)} + \frac{1}{r\sigma_t^2}\frac{\partial}{\partial r}\frac{\phi^{(0)}}{2}\sum_{m=1}^{M}\mu_m\left[\alpha_{m+\frac{1}{2}}\mu_{m+\frac{1}{2}} - \alpha_{m-\frac{1}{2}}\mu_{m-\frac{1}{2}}\right] . \qquad (40)$$

If the second term on the right hand side of Eq. (40) is zero, then $J^{(2)}$ satisfies Fick's law, and, consequently, the first-order flux will satisfy the correct diffusion equation. Eqs. (34) and (40) fully define our diffusion equation for the first-order flux and are in agreement with Eq. (6) if the second term in Eq. (40) is zero.

In order for Fick's law in Eq. (40) to be correct, the following equation must be satisfied

$$\sum_{m=1}^{M}\mu_m\left[\alpha_{m+\frac{1}{2}}\mu_{m+\frac{1}{2}} - \alpha_{m-\frac{1}{2}}\mu_{m-\frac{1}{2}}\right] = 0 \ . \qquad (41)$$

This summation is the same expression that Morel and Montry called β and forced to zero in order to preserve the Galerkin diffusion approximation. Using the asymptotic approach to the diffusion limit, we have shown that the leading-order flux is accurate for all angular discretizations. However, Eq. (41) is not satisfied by the step and diamond discretizations, resulting in a first-order error in the diffusion limit. The error in the diffusion limit for the step and diamond discretizations is introduced in the expression for the second-order current given by Eq. (40), which couples the leading-order flux to the

first-order flux. The Galerkin approach is unable to uncover the source of the error with the same amount of detail as the asymptotic approach.

Morel and Montry have shown that Eq. (41) is satisfied assuming the following weighted diamond weighting factors

$$\tau_m = \frac{\mu_m - \mu_{m-\frac{1}{2}}}{\mu_{m+\frac{1}{2}} - \mu_{m-\frac{1}{2}}} \ . \tag{42}$$

It is easy to show that these weighting factors are uniquely defined by the weighted diamond relationship between the cell-center and cell-edge cosines

$$\mu_m = \tau_m \mu_{m+\frac{1}{2}} + \left(1-\tau_m\right)\mu_{m-\frac{1}{2}} \ . \tag{43}$$

Equation (43) implies that Eq. (15) will exactly relate the cell-edge and cell-center fluxes when the angular flux assumes the linear form defined by Eq. (1).

To provide an example, we first look at the S_2 case, where there are two quadrature directions, a starting direction, an ending direction, and one interpolated direction as shown in Fig. 1. We next expand the summation given in Eq. (41).

$$\begin{aligned} &\sum_{m=1}^{2} \mu_m \left[\alpha_{m+\frac{1}{2}} \mu_{m+\frac{1}{2}} - \alpha_{m-\frac{1}{2}} \mu_{m-\frac{1}{2}} \right] \\ &= \mu_1 \left[\alpha_{\frac{3}{2}} \mu_{\frac{3}{2}} - \alpha_{\frac{1}{2}} \mu_{\frac{1}{2}} \right] + \mu_2 \left[\alpha_{\frac{5}{2}} \mu_{\frac{5}{2}} - \alpha_{\frac{3}{2}} \mu_{\frac{3}{2}} \right] \end{aligned} \tag{44}$$

In order for this summation to be zero,

$$\alpha_{\frac{3}{2}} \mu_{\frac{3}{2}} \left(\mu_1 - \mu_2\right) = 0 \ . \tag{45}$$

As a result, in order for the first-order flux to satisfy a diffusion equation,

$$\mu_{3/2} = 0 \ . \tag{46}$$

This interpolated value of μ causes the τ values in Eq. (42) to equal

$$\begin{aligned} \tau_1 &= \mu_1 + 1 \\ \tau_2 &= \mu_2 \ . \end{aligned} \tag{47}$$

A simple average relationship, where all τ values equal ½, would force the quadrature set to be the midpoint rule, $\mu_1 = -1/2$, $\mu_2 = 1/2$. However, the midpoint rule is not a good choice of quadrature sets in general. If we want to use a general quadrature set and preserve the ability of the angular discretization to satisfy the correct diffusion equation with the first-order flux, we must use the Morel and Montry weighted diamond weighting factors for the angular flux given in Eq. (42).

We note a few more properties of the step and diamond discretizations. First, as the number of quadrature points is increased with these methods, their respective solutions approach the correct diffusive behavior through first order. This occurs because the sum in Eq. (41) approaches zero as the number of quadrature points becomes large. In TABLE I we have calculated the value of this sum for the Morel and Montry weighted diamond differencing scheme (MM WDD), the step differencing scheme (SD), and the diamond differencing scheme (DD) for different orders of the Gauss-Legendre quadrature set. As expected, the Morel and Montry weighted diamond scheme yields a sum that is zero to round-off, while the step and diamond difference schemes yield a sum that approaches zero as the quadrature order is increased.

5. The Asymptotic Analysis for RZ geometry

The RZ transport equation with isotropic scattering and an isotropic distributed source is written in conservation form[1] as

$$\frac{\mu}{r}\frac{\partial}{\partial r}r\psi(r,z,\omega,\xi)-\frac{1}{r}\frac{\partial}{\partial\omega}\eta\ \ (\psi,z,\ \omega,\ )+\xi\ \ \frac{\partial}{\partial z}\ \ (\psi,z,\ \omega,\ )+\xi\ \ _t(\sigma,z)\psi(r,\omega,\ \ ,\xi)$$
$$=\frac{1}{4\pi}\sigma_s(r,z)\phi(r,z)+\frac{1}{4\pi}Q(r,z)\ . \tag{48}$$

The coordinate system corresponding to this equation is shown in Fig. 2, where $\xi=\cos\theta$ $\mu=\sin\theta\cos\omega$, $\eta=\sin\theta\sin\omega$ in Eq. (48). We now apply a S_n angular discretization to Eq. (48), resulting in

$$\frac{\mu_{m,n}}{r}\frac{\partial}{\partial r}r\psi_{m,n}(r,z)+\frac{\alpha_{m+1/2,n}\psi_{m+1/2,n}(r,z)-\alpha_{m-1/2,n}\psi_{m-1/2,n}(r,z)}{rw_{m,n}}+$$
$$\xi_{m,n}\frac{\partial}{\partial z}\psi_{m,n}(r,z)+\sigma_t\psi_{m,n}(r,z)=\frac{1}{4\pi}\sigma_s\phi(r,z)+\frac{1}{4\pi}Q\ , \tag{49}$$

where

$$\alpha_{m+1/2,n}=\alpha_{m+1/2,n}-\mu_{m,n}w_{m,n}\ ,$$
$$\alpha_{1/2,n}=\alpha_{M+1/2,n}=0\ , \tag{50}$$

and

$$\sum_{n=1}^{N}\sum_{m=1}^{M_n}w_{m,n}=4\pi\ ,$$
$$\phi(r,z)=\sum_{n=1}^{N}\sum_{m=1}^{M_n}w_{m,n}\psi_{m,n}(r,z)\ , \tag{51}$$
$$\vec{J}(r,z)=\sum_{n=1}^{N}\sum_{m=1}^{M_n}w_{m,n}\vec{\Omega}_{m,n}\psi_{m,n}(r,z)\ .$$

The index n is the ξ-level index, M_n is the number of directions on each ξ-level, and N is the number of ξ-levels. All of the directions on a given ξ-level have the same ξ-cosine.

The starting directions, weighted directions, and ξ-levels for an octant of a S_6 triangular quadrature set are illustrated in Fig. 3. The cell-edge cosines associated with Eq. (49) are obtained as in the spherical geometry case except that there is a separate recursion and starting cosine for each ξ-level

$$\begin{aligned} \mu_{m+\frac{1}{2},n} &= \mu_{m+\frac{1}{2},n} + \tilde{w}_{m,n} \quad , \\ \mu_{\frac{1}{2},n} = -\sqrt{1-\xi_n^2} \ , \ \mu_{M+\frac{1}{2},n} &= +\sqrt{1-\xi_n^2} \ , \end{aligned} \tag{52}$$

where the weights in Eq. (52) are normalized on each level to sum to $2\sqrt{1-\xi_n^2}$. While $\mu_{\frac{1}{2},n}$ is explicitly set to $-\sqrt{1-\xi_n^2}$ to start the recursion, $\mu_{M+\frac{1}{2},n}$ will always be equal to $+\sqrt{1-\xi_n^2}$ when computed recursively. To complete this angular discretization, we assume a general weighted diamond relationship between the cell-edge and cell-center cosines on each ξ-level:

$$\psi_{m,n} = \tau_{m,n}\psi_{m+\frac{1}{2},n} + \left(1-\tau_{m,n}\right)\psi_{m-\frac{1}{2},n} \quad , \tag{53}$$

where the weighting factors can take on any value between zero and one. As in the spherical geometry case, $\tau_{m,n}$=1 gives the step scheme and $\tau_{m,n}$=1/2 gives the diamond scheme. Solving Eq. (53) for $\psi_{m+1/2,n}$, we get

$$\psi_{m+\frac{1}{2},n} = \frac{1}{\tau_{m,n}}\psi_{m,n} - \frac{(1-\tau_{m,n})}{\tau_{m,n}}\psi_{m-\frac{1}{2},n} \quad . \tag{54}$$

Equation (54) is a recursion that needs a starting flux on each ξ-level, $\psi_{1/2,n}$. Following Eq. (52), we find that the cosine corresponding to the starting value on level n is $\mu_{\frac{1}{2},n} = -\sqrt{1-\xi_n^2}$. It is easily shown that the flux along this direction satisfies the following Cartesian equation

$$-\left(1-\xi_n\right)^{1/2}\frac{\partial}{\partial r}\psi_{1/2,n}\left(r,z\right)+\xi_n\frac{\partial}{\partial z}\psi_{1/2,n}\left(r,z\right)+\sigma_t\left(r,z\right)\psi_{1/2,n}\left(r,z\right)$$
$$=\frac{1}{4\pi}\sigma_s\left(r,z\right)\phi(r,z)+\frac{1}{4\pi}Q\ . \tag{55}$$

Finally, we assume a standard S_n quadrature set that possesses ξ-levels, symmetry about the μ–η and ξ–η planes, and integrates all polynomials in the direction cosines through second (quadratic) order.

We begin the asymptotic analysis by applying the appropriate scaling to Eqs. (49) and (55). The RZ transport equation becomes

$$\frac{\mu_{m,n}}{r}\frac{\partial}{\partial r}r\psi_{m,n}\left(r,z\right)+\frac{\alpha_{m+1/2,n}\psi_{m+1/2,n}\left(r,z\right)-\alpha_{m-1/2,n}\psi_{m-1/2,n}\left(r,z\right)}{rw_{m,n}}+$$
$$\xi_{m,n}\frac{\partial}{\partial z}\psi_{m,n}\left(r,z\right)+\frac{\sigma_t}{\varepsilon}\psi_{m,n}\left(r,z\right)=\frac{1}{4\pi}\left(\frac{\sigma_t}{\varepsilon}-\varepsilon\sigma_a\right)\phi\left(r,z\right)+\frac{1}{4\pi}\varepsilon Q\ , \tag{56}$$

and the starting-direction equation becomes

$$-\left(1-\xi_n\right)^{1/2}\frac{\partial}{\partial r}\psi_{1/2,n}\left(r,z\right)+\xi_n\frac{\partial}{\partial z}\psi_{1/2,n}\left(r,z\right)+\frac{\sigma_t}{\varepsilon}\psi_{1/2,n}\left(r,z\right)$$
$$=\frac{1}{4\pi}\left(\frac{\sigma_t}{\varepsilon}-\varepsilon\sigma_a\right)\phi(r,z)+\frac{1}{4\pi}\varepsilon Q\ . \tag{57}$$

We then substitute our flux guesses from Eq. (3) into Eqs. (56) and (57). This results in

$$\frac{\mu_{m,n}}{r}\frac{\partial}{\partial r}r\left[\psi_{m,n}{}^{(0)}+\varepsilon\psi_{m,n}{}^{(1)}+\varepsilon^2\psi_{m,n}{}^{(2)}\ldots\right]$$
$$+\frac{\alpha_{m+1/2,n}\left[\psi^{(0)}_{m+1/2,n}+\varepsilon\psi^{(1)}_{m+1/2,n}+\varepsilon^2\psi^{(2)}_{m+1/2,n}\cdot\ \right]-\alpha_{m-1/2,n}\left[\psi^{(0)}_{m-1/2,n}+\varepsilon\psi^{(1)}_{m-1/2,n}+\varepsilon^2\psi^{(2)}_{m-1/2,n}\ \cdot\right]}{rw_{m,n}}$$
$$+\xi_{m,n}\frac{\partial}{\partial z}\left[\psi_{m,n}{}^{(0)}+\varepsilon\psi_{m,n}{}^{(1)}+\varepsilon^2\psi_{m,n}{}^{(2)}\ldots\right]+\frac{\sigma_t}{\varepsilon}\left[\psi_{m,n}{}^{(0)}+\varepsilon\psi_{m,n}{}^{(1)}+\varepsilon^2\psi_{m,n}{}^{(2)}\ldots\right]$$
$$=\frac{1}{4\pi}\left(\frac{\sigma_t}{\varepsilon}-\varepsilon\sigma_a\right)\left[\phi^{(0)}+\varepsilon\phi^{(1)}+\varepsilon^2\phi^{(2)}\ldots\right]+\frac{1}{4\pi}\varepsilon Q\ , \tag{58}$$

and

$$-\left(1-\xi_n\right)^{1/2}\frac{\partial}{\partial r}\left[\psi^{(0)}_{1/2\,n}+\varepsilon\psi^{(1)}_{1/2\,n}+\varepsilon^2\psi^{(2)}_{1/2\,n}\ldots\right]+\xi_n\frac{\partial}{\partial z}\left[\psi^{(0)}_{1/2\,n}+\varepsilon\psi^{(1)}_{1/2,n}+\varepsilon^2\psi^{(2)}_{1/2,n}\ldots\right]$$
$$+\frac{\sigma_t}{\varepsilon}\left[\psi^{(0)}_{1/2,n}+\varepsilon\psi^{(1)}_{1/2,n}+\varepsilon^2\psi^{(2)}_{1/2,n}\ldots\right] \tag{59}$$
$$=\frac{1}{4\pi}\left(\frac{\sigma_t}{\varepsilon}-\varepsilon\sigma_a\right)\left[\phi^{(0)}+\varepsilon\phi^{(1)}+\varepsilon^2\phi^{(2)}\ldots\right]+\frac{1}{4\pi}\varepsilon Q\ .$$

As in the spherical geometry case, we collect and equate like order terms in Eqs. (58) and (59) to produce relationships that describe the individual modes of the angular and scalar flux. Using the same logic as in the spherical geometry case the *O(1/ε)* terms imply that the leading-order angular flux is isotropic,

$$\psi^{(0)}=\frac{1}{4\pi}\phi^{(0)}\ , \tag{60}$$

which is in agreement with Eq. (4).

After some algebra, the *O(1)* relationship generated by Eq. (58) is

$$\vec{\Omega}_{m,n}\vec{\nabla}\frac{\phi^{(0)}}{4\pi}+\sigma_t\psi^{(1)}_{m,n}=\frac{1}{4\pi}\sigma_t\phi^{(1)}, \tag{61}$$

where

$$\vec{\Omega}_{m,n}=\mu_{m,n}\mathbf{e_r}+\xi_{m,n}\mathbf{e_z}\ ,$$
$$\vec{\nabla}=\frac{\partial}{\partial r}\mathbf{e_r}+\frac{\partial}{\partial z}\mathbf{e_z}\ . \tag{62}$$

As in the 1D spherical case, taking the zeroth moment of Eq. (61) will demonstrate that the solvability condition is satisfied. We then use Eq. (61) to find the first-order current by taking the first angular moment of the equation and applying standard quadrature properties and the definitions given in Eq. (51). The first-order current is

$$\vec{J}^{(1)} = -\frac{1}{3\sigma_t}\vec{\nabla}\phi^{(0)} \quad , \tag{63}$$

which is the expected Fick's law relationship between first-order current and leading-order flux.

We now collect the *O(ε)* terms in Eq. (58), resulting in

$$\begin{aligned} &\frac{\mu_{m,n}}{r}\frac{\partial}{\partial r}r\psi^{(1)}_{m,n} + \frac{\alpha_{m+\frac{1}{2},n}\psi^{(1)}_{m+\frac{1}{2},n} - \alpha_{m-\frac{1}{2},n}\psi^{(1)}_{m-\frac{1}{2},n}}{rw_{m,n}} + \xi_{m,n}\frac{\partial}{\partial z}\psi^{(1)}_{m,n} \\ &+\sigma_t\psi^{(2)}_{m,n} = \frac{1}{4\pi}\sigma_t\phi^{(2)} - \frac{1}{4\pi}\sigma_a\phi^{(0)} + \frac{1}{4\pi}Q \quad . \end{aligned} \tag{64}$$

We take the zeroth moment of this relationship, and perform some algebra. This process results in an equation involving the first-order current and zeroth-order scalar flux:

$$\frac{1}{r}\vec{\nabla}\cdot r\vec{J}^{(1)} + \sigma_a\phi^{(0)} = Q \quad . \tag{65}$$

Substituting our Fick's law relationship into Eq. (65), we obtain

$$-\frac{1}{r}\vec{\nabla}\cdot r\frac{1}{3\sigma_t}\vec{\nabla}\phi^{(0)} + \sigma_a\phi^{(0)} = Q \quad . \tag{66}$$

Equation (66) is in agreement with Eq. (5) and shows that the correct diffusion equation is satisfied by the leading-order flux. As in spherical geometry, this result is true for any choice of weighting factors in the approximation of the angular flux.

We will now determine what weighted diamond weighting factors will cause the angular discretization to satisfy the correct first-order flux diffusion equation. To do this, we will follow essentially the same procedure as in the 1D spherical case. This procedure involves six steps.

1. Collect the $O(\varepsilon^2)$ terms in Eq. (58).
2. Take the zeroth angular moment of the resultant equation in step 1. This zeroth moment produces a relationship between the second-order current and the first-order scalar flux.
3. From Eq. (61) solve for the first-order angular flux ($\psi_{m,n}^{(1)}$), and substitute this relationship into Eq. (64), the $O(\varepsilon)$ equation.
4. Take the first angular moment of the equation generated in step 3.
5. Simplify the first angular moment equation using standard quadrature properties, the definitions of the α-coefficients, and algebra.
6. Use the equation generated in step 5 to solve for the second-order current, $\vec{J}^{(2)}$, in terms of the first-order scalar flux. Note that if the second-order current satisfies Fick's Law in terms of the first-order scalar flux, then we will have shown that the first-order flux is described by the diffusion equation. This diffusion equation is determined from the results of step 2 and step 6.

In step 2, the zeroth angular moment of the $O(\varepsilon^2)$ equation is

$$\frac{1}{r}\vec{\nabla}\cdot r\vec{J}^{(2)} + \sigma_a \phi^{(1)} = 0 \ . \tag{67}$$

The relationship for the second-order current in step 6 is

$$\vec{J}^{(2)} = -\frac{1}{3\sigma_t}\left(\frac{\partial}{\partial r}\phi^{(1)} + \frac{\partial}{\partial z}\phi^{(1)}\right)$$
$$+\frac{1}{\sigma_t^2 r}\frac{\partial\phi^{(0)}}{\partial r}\sum_{n=1}^{N}\sum_{m=1}^{M_n}\left(\mu_{m,n}+\xi_{m,n}\right)\left(\alpha_{m+\frac{1}{2},n}\mu_{m+\frac{1}{2},n} - \alpha_{m-\frac{1}{2},n}\mu_{m-\frac{1}{2},n}\right) \tag{68}$$
$$+\frac{1}{\sigma_t^2 r}\frac{\partial\phi^{(0)}}{\partial z}\sum_{n=1}^{N}\sum_{m=1}^{M_n}\left(\mu_{m,n}+\xi_{m,n}\right)\left(\alpha_{m+\frac{1}{2},n}\xi_{m+\frac{1}{2},n} - \alpha_{m-\frac{1}{2},n}\xi_{m-\frac{1}{2},n}\right) .$$

Equations (67) and (68) are analogous to Eqs. (34) and (40) from the spherical geometry analysis. The Appendix contains a more detailed description of the six steps to generate these relationships for RZ geometry.

In order for the second-order current and first-order flux to be related by Fick's Law, the following terms of Eq. (68) must be satisfied:

$$\begin{aligned}
&\sum_{n=1}^{N}\sum_{m=1}^{M_n}\left(\mu_{m,n}+\xi_{m,n}\right)\left(\alpha_{m+\frac{1}{2},n}\mu_{m+\frac{1}{2},n} - \alpha_{m-\frac{1}{2},n}\mu_{m-\frac{1}{2},n}\right) = 0 \ , \\
&\sum_{n=1}^{N}\sum_{m=1}^{M_n}\left(\mu_{m,n}+\xi_{m,n}\right)\left(\alpha_{m+\frac{1}{2},n}\xi_{m+\frac{1}{2},n} - \alpha_{m-\frac{1}{2},n}\xi_{m-\frac{1}{2},n}\right) = 0 \ .
\end{aligned} \tag{69}$$

It is easy to show that the second relationship in Eq. (69) is zero because $\xi_{m-\frac{1}{2},n} = \xi_{m+\frac{1}{2},n} = \xi_{m,n}$. In particular,

$$\begin{aligned}
&\sum_{n=1}^{N}\sum_{m=1}^{M_n}\left(\mu_{m,n}+\xi_{m,n}\right)\left(\alpha_{m+\frac{1}{2},n}\xi_{m+\frac{1}{2},n} - \alpha_{m-\frac{1}{2},n}\xi_{m-\frac{1}{2},n}\right) \\
&= -\sum_{n=1}^{N}\sum_{m=1}^{M_n}\left(\mu_{m,n}+\xi_{m,n}\right)\xi_{m,n}\mu_{m,n} \ , \\
&= -\sum_{n=1}^{N}\sum_{m=1}^{M_n}\left(\mu_{m,n}^2\xi_{m,n} + \mu_{m,n}\xi_{m,n}^2\right) \\
&= 0 \ .
\end{aligned} \tag{70}$$

The first relationship in Eq. (69) is more difficult to simplify. First we expand it as follows

$$\sum_{n=1}^{N}\sum_{m=1}^{M_n}\left(\mu_{m,n}+\xi_{m,n}\right)\left(\alpha_{m+\frac{1}{2},n}\mu_{m+\frac{1}{2},n}-\alpha_{m-\frac{1}{2},n}\mu_{m-\frac{1}{2},n}\right)=$$
$$\sum_{n=1}^{N}\sum_{m=1}^{M_n}\mu_{m,n}\left(\alpha_{m+\frac{1}{2},n}\mu_{m+\frac{1}{2},n}-\alpha_{m-\frac{1}{2},n}\mu_{m-\frac{1}{2},n}\right)+ \tag{71}$$
$$\sum_{n=1}^{N}\sum_{m=1}^{M_n}\xi_{m,n}\left(\alpha_{m+\frac{1}{2},n}\mu_{m+\frac{1}{2},n}-\alpha_{m-\frac{1}{2},n}\mu_{m-\frac{1}{2},n}\right),$$

and then note that the second term in Eq. (71) is zero because the quadrature set contains symmetric levels. This means that for every $\xi_{m,n}$ level that contains a series of $\mu_{m,n}$, $\mu_{m+\frac{1}{2},n}$, and $\mu_{m-\frac{1}{2},n}$ values there is another ξ-level with the same series of $\mu_{m,n}$, $\mu_{m+\frac{1}{2},n}$, and $\mu_{m-\frac{1}{2},n}$ values but with an opposite sign of $\xi_{m,n}$. As a result,

$$\sum_{n=1}^{N}\sum_{m=1}^{M_n}\xi_{m,n}\left(\alpha_{m+\frac{1}{2},n}\mu_{m+\frac{1}{2},n}-\alpha_{m-\frac{1}{2},n}\mu_{m-\frac{1}{2},n}\right)=0\ , \tag{72}$$

and the second-order current becomes

$$\vec{J}^{(2)}=-\frac{1}{3\sigma_t}\left(\frac{\partial}{\partial r}\phi^{(1)}+\frac{\partial}{\partial z}\phi^{(1)}\right)$$
$$+\frac{1}{\sigma_t^2 r}\sum_{n=1}^{N}\sum_{m=1}^{M_n}\mu_{m,n}\left(\alpha_{m+\frac{1}{2},n}\mu_{m+\frac{1}{2},n}-\alpha_{m-\frac{1}{2},n}\mu_{m-\frac{1}{2},n}\right)\frac{\partial\phi^{(0)}}{\partial r}\ . \tag{73}$$

If the second term on the right hand side of Eq. (73) is zero, we will have a correct Fick's Law relationship for the second-order current. The sum in Eq. (73) is completely analogous to Eq. (41) from the spherical geometry case. For this reason, we can draw the same conclusion as in the spherical geometry case. This term will be zero if we use the Morel and Montry weighting factors in Eq. (53) analogous to those defined by Eq. (42):

$$\tau_{m,n}=\frac{\mu_{m,n}-\mu_{m-\frac{1}{2},n}}{\mu_{m+\frac{1}{2},n}-\mu_{m-\frac{1}{2},n}}\ . \tag{74}$$

Thus, if we use the weighting factors given in Eq. (74), we will achieve first order consistency in the diffusion limit, and the combination of Eqs. (67) and (73) are in agreement with Eq. (6).

The sum in Eq. (71) will approach zero in the step and diamond differencing cases as the number of quadrature points becomes large. This result means that the step and diamond differencing solutions actually do approach the correct diffusion limit through first order as the angular approximation becomes infinitely refined. In TABLE II we have calculated the value of this sum for the Morel and Montry weighted diamond differencing case and the diamond differencing case for different orders of the Level Symmetric quadrature set. As expected, the Morel and Montry weighted diamond scheme yields a sum that is zero to round-off, while the diamond difference scheme yields a sum that approaches zero as the quadrature order is increased.

The results of the asymptotic analysis through first order are fundamentally the same for the spherical and cylindrical geometry cases. In both cases, a contamination term appears in the expression for the second-order current (Eq. (40) for spherical geometry and Eq. (73) for cylindrical geometry). In particular, the second-order current can be described as follows

$$\begin{aligned}
&\vec{J}^{(2)} = -\frac{1}{3\sigma_t}\vec{\nabla}\phi^{(1)} + \frac{\beta}{r\sigma_t^2}\frac{\partial}{\partial r}\phi^{(0)}, \\
&\beta_{spherical} = \frac{1}{2}\sum_{m=1}^{M}\mu_m\left[\alpha_{m+1/2}\mu_{m+1/2} - \alpha_{m-1/2}\mu_{m-1/2}\right], \\
&\beta_{cylindrical} = \sum_{n=1}^{N}\sum_{m=1}^{M}\mu_m\left[\alpha_{m+1/2,n}\mu_{m+1/2,n} - \alpha_{m-1/2,n}\mu_{m-1/2,n}\right],
\end{aligned} \tag{75}$$

where the contamination term is multiplied by the β factor. This is the same factor that Morel and Montry forced to be zero to preserve the Galerkin diffusion approximation. Forcing this β factor to be zero determines the Morel and Montry weighting factors for the weighted diamond difference discretization. Furthermore, the contamination term only affects the accuracy of the first-order flux diffusion discretization. As a result, all three angular discretizations are accurate when a problem is sufficiently thick and diffusive such that the leading-order solution dominates.

Often, the error due to the contamination term in the first-order equation presents itself as a flux dip in problems not sufficiently thick and diffusive. The flux dip means that the flux solution has an unphysical *positive* slope at the origin of the sphere or cylinder. However, as first shown by Morel and Montry, this error can also manifest itself as an unphysical *negative* slope at the origin of the sphere or cylinder. This negative slope solution does not produce a flux dip but rather a different form of anomalous flux shape . A preliminary investigation indicates that our asymptotic analysis can be extended to predict the slope of the flux due to the error in the solution caused by the β term. However computational testing of this extension is extremely problematic because the theory only rigorously applies when the solution is completely dominated by the asymptotic solution to first order. Such domination only occurs when the solution is highly diffusive and the flux dip is essentially negligible. Furthermore, preliminary computational results indicate that contributions from the higher-order asymptotic terms, which rapidly decay when the Morel and Montry weighted diamond scheme is used, persist to much smaller values of ε when the step and diamond schemes

are used. This greatly exacerbates the difficulty of computational testing and indicates the presence of large higher order contamination terms for the step and diamond schemes. Thus we conjecture that a practical prediction of the slope of the flux at the origin will require a higher-order analysis. Such an analysis is beyond the scope of this paper, and will not be further discussed.

The Galerkin diffusion analysis of Montry and Morel was unable to pinpoint the cause of the error associated with the step and diamond schemes to the level of detail that the asymptotic analysis reveals. The purpose of the Galerkin analysis was to determine the correct angular discretization that would eliminate the flux dip when the diffusion approximation was valid. This was done with the expectation that it would also eliminate the flux dip in general. It was computationally determined that preservation of the Galerkin diffusion approximation did in fact eliminate the flux dip in general. The Morel and Montry weighted diamond method that was derived is the only method in the family of general weighted diamond methods (which includes the step and diamond schemes) that forces the β factor to be zero for any standard quadrature set. However, the Galerkin approach was unable to show that all methods are accurate in extremely diffusive problems. The asymptotic approach reveals this property of the methods because it represents a true analysis of the diffusion limit and the approach to the diffusion limit.

6. Numerical Test Problems

We have run a variety of test problems to demonstrate the inaccuracy created by the methods which do not produce accurate asymptotic behavior through first order. We demonstrate this inaccuracy by showing anomalous and unphysical slopes in the scalar flux at the origin of the sphere or cylinder. This unphysical behavior of the step and diamond differencing methods is caused by their inconsistency to the analytic transport equation through first order. We ran these test problems using Capsaicin[5], a transport software project being developed at Los Alamos National Laboratory. All of these problems share the following properties.

Radius = 1.0
Height of Cylinder = 1.0 (for RZ only)
$\sigma_t = 0.1$
$\sigma_a = 0.05$
$Q = 1.0$

The boundary conditions are reflecting at the origin of the radial coordinates and vacuum elsewhere. Capsaicin uses a linear discontinuous finite element spatial discretization for 1D spherical geometry and a bi-linear discontinuous finite element spatial discretization applied to a uniform rectangular grid in RZ geometry. We ensured that all numerical solutions presented are spatially converged.

For each problem, we choose a scaling factor, ε, that scales the above data in the same manner of the diffusion scaling: $\sigma_t \to \frac{\sigma_t}{\varepsilon}$, $\sigma_a \to \varepsilon\ \sigma_a$, $Q \to \varepsilon Q$. As ε becomes small, the problem becomes diffusive. In each of our plots, we plot the scalar flux

divided by the scalar flux at the origin. This normalization of the flux will better show the slope of the scalar flux at the origin. The flux at the origin should be the maximum value of the curve, so if the curve for a particular ε-value becomes greater than one, the solution exhibits a flux dip, or positive slope at the origin. The flux can be maximum at the origin and still be incorrect. This unphysicality, or error, in the flux will be manifested as a negative slope in the flux at the origin, and we correlate this unphysicality to a lack of consistency with the diffusion limit through first order.

In Fig. 4 and Fig. 5 we show results for an $\varepsilon=1$ problem using a S_2 quadrature set in spherical geometry. The flux dip, or positive slope of the flux at the origin, is evident for the diamond differencing case in Fig. 4. Furthermore, we see that the slope of the flux at the origin is zero for the Morel and Montry weighted diamond differencing, as predicted by the analysis. In Fig. 5, we observe a negative slope at the origin for the scalar flux in the step differencing case, which Morel and Montry predicted because β is positive for the S_2 step case as shown in TABLE I. The result from this particular test problem appears to be an anomalous linear solution for step differencing. We have verified that this linear shape is in fact the correct solution for the $\varepsilon=1$, S_2 test problem with step differencing. Because ε is not small for this problem, it is not diffusive. As a result, the leading-order scalar flux does not completely dominate the solution and we see the result of the error in the first-order flux for the both the step and diamond differencing cases.

In Fig. 6 and Fig. 7, we have plotted the step and diamond difference schemes respectively for our test problem in spherical geometry as $\varepsilon \to 0$ for the multiple values of ε. Fig. 6 shows that the negative slope at the origin becomes less severe as $\varepsilon \to 0$, and that the step differencing solution actually begins to have some curvature. However, this plot indicates that even for small values of ε, we will still see an error in the flux. Fig. 7 shows that when $\varepsilon \to 0$, the flux dip disappears for the angular diamond differencing, which is what we expect because the leading-order solution begins to dominate in the diffusion limit. In Fig. 8, we have plotted the same set of ε curves, but for the Morel and Montry weighted diamond angular discretization. For this discretization, every flux has a zero slope at the origin, which confirms the results of the asymptotic analysis. From this series of figures we conclude that the Morel and Montry weighted diamond angular discretization is extremely accurate for all values of ε, diamond differencing becomes accurate as the problems becomes more diffusive, and the step differencing requires an extremely diffusive problem to be accurate. It is interesting to note that step differencing is extremely inaccurate for these problems even compared with diamond differencing.

We ran similar test problems for the RZ geometry case. Fig. 9 demonstrates that the Morel and Montry weighted diamond angular discretization exhibits no unphysical behavior in the flux at the origin for all values of ε in RZ geometry. In Fig. 10 we note the flux dip, or positive slope in the flux, near the origin for the diamond angular differencing. This plot shows that as $\varepsilon \to 0$, the problem becomes more diffusive, the flux dip disappears, just as in spherical geometry, further confirming the results of the asymptotic analysis.

In Fig. 11 and Fig. 12, we have plotted the ε=1 case for a variety of quadrature orders for the diamond differencing angular discretization in 1D spherical and RZ geometries respectively. In each figure, the flux dip appears for each quadrature order, but diminishes as the quadrature order increases. We note that in TABLE I and TABLE II the β sums are approaching zero as the quadrature order approaches infinity.

7. Comparison of the Galerkin and Asymptotic Analyses

The primary conclusion from the Galerkin analysis for the general family of weighted diamond discretization schemes was that there was only one particular weighted diamond scheme that yielded a zero value for the β factor and thereby preserved the Galerkin diffusion approximation. This ensured that there would be no flux dip when the Galerkin approximation was valid, and suggested that the flux dip might be eliminated for all problems. The general elimination of the flux dip was computationally confirmed. A problem with this analysis is that it gives no information as to the conditions under which the Galerkin approximation will be valid. Furthermore, when the Galerkin approximation is not preserved by a scheme, the Galerkin analysis only yields information on the behavior of the S_n solution under the assumption that the angular flux has a linear angular dependence. Such dependence is only guaranteed for S_2 quadrature in 1D spherical geometry with step differencing, thereby severely limiting the predictive capability of the Galerkin analysis when the Galerkin diffusion approximation is not preserved.

The asymptotic approach to the diffusion limit analysis yields much more information because it makes no assumptions about the dependence of the angular flux. Rather it assumes a certain physical scaling of the S_n equations that leads to the validity of the diffusion approximation in the limit as the scaling parameter approaches zero. This analysis reveals that for any weighted diamond angular differencing scheme, the leading-order scalar flux will satisfy the correct diffusion equation. As a result, when a problem is truly diffusive, and thus dominated by the leading-order solution, any relationship between the angular fluxes with the correct starting direction equation will produce accurate solutions. The Galerkin approach to this analysis was unable to predict this very important behavior, which we have demonstrated in numerous test problems. Furthermore, the asymptotic approach reveals that the β factor appears as a contamination term in the expression for the second-order current. This second-order current affects the first-order scalar flux, which prevents the first-order scalar flux from being described by the correct diffusion equation. As a result, if the problem is approaching the diffusion limit, but not completely dominated by the leading-order solution, we will see the effect of this contamination term in the form of a non-zero slope in the scalar flux at the origin of the problem. When the slope of the flux is positive, we will observe a flux dip in the solution; and when it is negative, we will observe a different form of anomalous flux shape

Our asymptotic analysis reveals that the Morel and Montry weighted diamond difference discretization is the only angular discretization in this family of methods that is

correct through first order in the asymptotic diffusion limit. We have shown that the step and diamond difference discretizations have a contamination term, which arises through a non-zero value of β, in the equation for the first-order scalar flux.

8. Conclusion

Using an asymptotic analysis, we have shown that the weighted diamond angular differencing scheme of Morel and Montry preserves the diffusion limit through first-order. This is not particularly surprising given that this scheme also preserves the Galerkin approximation. However, our asymptotic analysis also shows that any general weighted diamond scheme, including the step and diamond schemes, preserves the diffusion limit to leading-order, and therefore yields accurate results in problems sufficiently diffusive to be dominated by the leading-order solution. This is a significant result that cannot be obtained from a Galerkin analysis. While it might appear that the asymptotic and Galerkin analyses are in conflict, we believe that this is not the case. Rather we conjecture that preservation of the Galerkin approximation is equivalent to preservation of the asymptotic diffusion limit through first order. The reasoning behind this conjecture is straightforward. Preservation of the Galerkin approximation requires that a scheme be able to accurately represent an angular flux solution with a linear dependence in the direction cosines. The asymptotic diffusion-limit analysis shows that the first-order component of the angular flux is indeed linear in the direction cosines, but the leading-order component is isotropic. Thus, it is not surprising that a scheme which accurately represents an isotropic solution but not a linear solution can be accurate in the

diffusion limit to leading order while having a first-order error term. The Galerkin analysis cannot address the leading-order behavior, but it does address the overall first-order behavior in a limited sense.

Appendix

We first collect all the $O(\varepsilon^2)$ terms in Eq. (58), and take the zeroth angular moment of the equation.

$$\begin{aligned}\sum_{n=1}^{N}\sum_{m=1}^{M_n} w_{m,n}\mu_{m,n}\frac{\partial}{\partial r}r\psi_{m,n}^{(2)} + r\sum_{n=1}^{N}\sum_{m=1}^{M_n} w_{m,n}\xi_{m,n}\frac{\partial}{\partial z}\psi_{m,n}^{(2)} \\ +\sum_{n=1}^{N}\sum_{m=1}^{M_n}\left(\alpha_{m+\frac{1}{2},n}\psi_{m+\frac{1}{2},n}^{(2)} - \alpha_{m-\frac{1}{2},n}^{(2)}\psi_{m-\frac{1}{2},n}\right) \\ +r\sigma_t\sum_{n=1}^{N}\sum_{m=1}^{M_n} w_{m,n}\psi_{m,n}^{(3)} = \frac{1}{4\pi}r\sigma_t\phi^{(3)}\sum_{n=1}^{N}\sum_{m=1}^{M_n} w_{m,n} - \frac{1}{4\pi}r\sigma_a\phi^{(1)}\sum_{n=1}^{N}\sum_{m=1}^{M_n} w_{m,n}\ .\end{aligned} \tag{A.1}$$

In analogy with the spherical case, Eq. (A.1) simplifies to

$$\frac{1}{r}\vec{\nabla}\cdot r\vec{J}^{(2)} + \sigma_a\phi^{(1)} = 0\ . \tag{A.2}$$

Also, as in the spherical case, if we can find a Fick's law relationship for $\vec{J}^{(2)}$ in terms of $\phi^{(1)}$, then we will have shown that the first-order flux satisfies a diffusion equation for our S_n angular discretization in RZ geometry. In order to develop this relationship, we use Eq. (61) to solve for $\psi_{m,n}^{(1)}$,

$$\psi_{m,n}^{(1)} = \frac{1}{4\pi}\phi^{(1)} - \frac{1}{\sigma_t}\vec{\Omega}_{m,n}\cdot\vec{\nabla}\frac{\phi^{(0)}}{4\pi}, \tag{A.3}$$

which can be expanded as

$$\psi_{m,n}^{(1)} = \frac{1}{4\pi}\phi^{(1)} - \frac{1}{\sigma_t}\mu_{m,n}\frac{\partial\phi^{(0)}}{\partial r} - \frac{1}{\sigma_t}\xi_{m,n}\frac{\partial\phi^{(0)}}{\partial z}\ , \tag{A.4}$$

We then substitute this relationship into the *O(ε)* equation, Eq. (64), resulting in

$$\begin{aligned}
&\frac{\mu_{m,n}}{r}\frac{\partial}{\partial r}r\left(\frac{1}{4\pi}\phi^{(1)}-\frac{1}{\sigma_t}\mu_{m,n}\frac{\partial\phi^{(0)}}{\partial r}-\frac{1}{\sigma_t}\xi_{m,n}\frac{\partial\phi^{(0)}}{\partial z}\right)\\
&+\xi_{m,n}\frac{\partial}{\partial z}\left(\frac{1}{4\pi}\phi^{(1)}-\frac{1}{\sigma_t}\mu_{m,n}\frac{\partial\phi^{(0)}}{\partial r}-\frac{1}{\sigma_t}\xi_{m,n}\frac{\partial\phi^{(0)}}{\partial z}\right)\\
&+\frac{\alpha_{m+\frac{1}{2},n}\left(\frac{1}{4\pi}\phi^{(1)}-\frac{1}{\sigma_t}\mu_{m+\frac{1}{2},n}\frac{\partial\phi^{(0)}}{\partial r}-\frac{1}{\sigma_t}\xi_{m+\frac{1}{2},n}\frac{\partial\phi^{(0)}}{\partial z}\right)}{rw_{m,n}}\\
&-\frac{\alpha_{m-\frac{1}{2},n}\left(\frac{1}{4\pi}\phi^{(1)}-\frac{1}{\sigma_t}\mu_{m-\frac{1}{2},n}\frac{\partial\phi^{(0)}}{\partial r}-\frac{1}{\sigma_t}\xi_{m-\frac{1}{2},n}\frac{\partial\phi^{(0)}}{\partial z}\right)}{rw_{m,n}}\\
&+\sigma_t\psi^{(2)}_{m,n}=\frac{1}{4\pi}\sigma_t\phi^{(2)}-\frac{1}{4\pi}\sigma_a\phi^{(0)}+\frac{1}{4\pi}Q\ .
\end{aligned}\tag{A.5}$$

In order to solve for $\vec{J}^{(2)}$, we take the first angular moment of Eq. (A.5).

$$\begin{aligned}
&\frac{1}{r}\frac{\partial}{\partial r}r\frac{1}{4\pi}\phi^{(1)}\sum_{n=1}^{N}\sum_{m=1}^{M_n}w_{m,n}\left(\mu_{m,n}^2+\mu_{m,n}\xi_{m,n}\right)+\frac{\partial}{\partial z}\frac{1}{4\pi}\phi^{(1)}\sum_{n=1}^{N}\sum_{m=1}^{M_n}w_{m,n}\left(\mu_{m,n}\xi_{m,n}+\xi_{m,n}^2\right)\\
&-\frac{1}{r}\frac{\partial}{\partial r}r\frac{1}{\sigma_t}\frac{\partial\phi^{(0)}}{\partial r}\sum_{n=1}^{N}\sum_{m=1}^{M_n}w_{m,n}\left(\mu_{m,n}^3+\mu_{m,n}^2\xi_{m,n}\right)\\
&-\frac{1}{r}\frac{\partial}{\partial r}r\frac{1}{\sigma_t}\frac{\partial\phi^{(0)}}{\partial z}\sum_{n=1}^{N}\sum_{m=1}^{M_n}w_{m,n}\left(\mu_{m,n}^2\xi_{m,n}+\mu_{m,n}\xi_{m,n}^2\right)\\
&-\frac{\partial}{\partial z}\frac{1}{\sigma_t}\frac{\partial\phi^{(0)}}{\partial r}\sum_{n=1}^{N}\sum_{m=1}^{M_n}w_{m,n}\left(\mu_{m,n}^2\xi_{m,n}+\mu_{m,n}\xi_{m,n}^2\right)-\frac{\partial}{\partial z}\frac{1}{\sigma_t}\frac{\partial\phi^{(0)}}{\partial z}\sum_{n=1}^{N}\sum_{m=1}^{M_n}w_{m,n}\left(\mu_{m,n}\xi_{m,n}^2+\xi_{m,n}^3\right)\\
&+\frac{1}{4\pi r}\phi^{(1)}\sum_{n=1}^{N}\sum_{m=1}^{M_n}\left(\mu_{m,n}+\xi_{m,n}\right)\left(\alpha_{m+\frac{1}{2},n}-\alpha_{m-\frac{1}{2},n}\right)\\
&-\frac{1}{\sigma_t r}\frac{\partial\phi^{(0)}}{\partial r}\sum_{n=1}^{N}\sum_{m=1}^{M_n}\left(\mu_{m,n}+\xi_{m,n}\right)\left(\alpha_{m+\frac{1}{2},n}\mu_{m+\frac{1}{2},n}-\alpha_{m-\frac{1}{2},n}\mu_{m-\frac{1}{2},n}\right)\\
&-\frac{1}{\sigma_t r}\frac{\partial\phi^{(0)}}{\partial z}\sum_{n=1}^{N}\sum_{m=1}^{M_n}\left(\mu_{m,n}+\xi_{m,n}\right)\left(\alpha_{m+\frac{1}{2},n}\xi_{m+\frac{1}{2},n}-\alpha_{m-\frac{1}{2},n}\xi_{m-\frac{1}{2},n}\right)\\
&+\sigma_t\sum_{n=1}^{N}\sum_{m=1}^{M_n}w_{m,n}\left(\mu_{m,n}+\xi_{m,n}\right)\psi^{(2)}_{m,n}\\
&=\left[\frac{1}{4\pi}\sigma_t\phi^{(2)}-\frac{1}{4\pi}\sigma_a\phi^{(0)}+\frac{1}{4\pi}Q\right]\sum_{n=1}^{N}\sum_{m=1}^{M_n}w_{m,n}\left(\mu_{m,n}+\xi_{m,n}\right)\ .
\end{aligned}\tag{A.6}$$

Using standard quadrature relationships and the definition of the current in Eq. (51), we find that Eq. (A.6) simplifies to

$$\begin{aligned}
&\frac{1}{r}\frac{\partial}{\partial r}r\frac{1}{3}\phi^{(1)}+\frac{\partial}{\partial z}\frac{1}{3}\phi^{(1)}\\
&+\frac{1}{4\pi r}\phi^{(1)}\sum_{n=1}^{N}\sum_{m=1}^{M_n}\left(\mu_{m,n}+\xi_{m,n}\right)\left(\alpha_{m+\frac{1}{2},n}-\alpha_{m-\frac{1}{2},n}\right)\\
&-\frac{1}{\sigma_t r}\frac{\partial\phi^{(0)}}{\partial r}\sum_{n=1}^{N}\sum_{m=1}^{M_n}\left(\mu_{m,n}+\xi_{m,n}\right)\left(\alpha_{m+\frac{1}{2},n}\mu_{m+\frac{1}{2},n}-\alpha_{m-\frac{1}{2},n}\mu_{m-\frac{1}{2},n}\right)\\
&-\frac{1}{\sigma_t r}\frac{\partial\phi^{(0)}}{\partial z}\sum_{n=1}^{N}\sum_{m=1}^{M_n}\left(\mu_{m,n}+\xi_{m,n}\right)\left(\alpha_{m+\frac{1}{2},n}\xi_{m+\frac{1}{2},n}-\alpha_{m-\frac{1}{2},n}\xi_{m-\frac{1}{2},n}\right)\\
&+\sigma_t\vec{J}^{(2)}=0\ .
\end{aligned}\tag{A.7}$$

We further simplify Eq. (A.7) by using the chain rule of differentiation on the first term and the definition of the α-coefficients given in Eq. (50) to obtain

$$\begin{aligned}
&\frac{1}{3}\frac{\partial}{\partial r}\phi^{(1)}+\frac{1}{3r}\phi^{(1)}+\frac{\partial}{\partial z}\frac{1}{3}\phi^{(1)}\\
&-\frac{1}{4\pi r}\phi^{(1)}\sum_{n=1}^{N}\sum_{m=1}^{M_n}w_m\left(\mu_{m,n}^2+\mu_{m,n}\xi_{m,n}\right)\\
&+\frac{1}{\sigma_t r}\frac{\partial\phi^{(0)}}{\partial r}\sum_{n=1}^{N}\sum_{m=1}^{M_n}\left(\mu_{m,n}+\xi_{m,n}\right)\left(\alpha_{m+\frac{1}{2},n}\mu_{m+\frac{1}{2},n}-\alpha_{m-\frac{1}{2},n}\mu_{m-\frac{1}{2},n}\right)\\
&+\frac{1}{\sigma_t r}\frac{\partial\phi^{(0)}}{\partial z}\sum_{n=1}^{N}\sum_{m=1}^{M_n}\left(\mu_{m,n}+\xi_{m,n}\right)\left(\alpha_{m+\frac{1}{2},n}\xi_{m+\frac{1}{2},n}-\alpha_{m-\frac{1}{2},n}\xi_{m-\frac{1}{2},n}\right)\\
&+\sigma_t\vec{J}^{(2)}=0\ .
\end{aligned}\tag{A.8}$$

We again use standard quadrature relationships to simplify Eq. (A.8) to

$$\begin{aligned}
&\frac{1}{3}\left(\frac{\partial}{\partial r}\phi^{(1)}+\frac{\partial}{\partial z}\phi^{(1)}\right)\\
&-\frac{1}{\sigma_t r}\frac{\partial\phi^{(0)}}{\partial r}\sum_{n=1}^{N}\sum_{m=1}^{M_n}\left(\mu_{m,n}+\xi_{m,n}\right)\left(\alpha_{m+\frac{1}{2},n}\mu_{m+\frac{1}{2},n}-\alpha_{m-\frac{1}{2},n}\mu_{m-\frac{1}{2},n}\right)\\
&-\frac{1}{\sigma_t r}\frac{\partial\phi^{(0)}}{\partial z}\sum_{n=1}^{N}\sum_{m=1}^{M_n}\left(\mu_{m,n}+\xi_{m,n}\right)\left(\alpha_{m+\frac{1}{2},n}\xi_{m+\frac{1}{2},n}-\alpha_{m-\frac{1}{2},n}\xi_{m-\frac{1}{2},n}\right)\\
&+\sigma_t\vec{J}^{(2)}=0\ .
\end{aligned}\tag{A.9}$$

If we solve for the second-order current in Eq. (A.9), the result is Eq. (68).

Acknowledgments

This work performed under the auspices of the U.S. Department of Energy by Lawrence Livermore National Laboratory under Contract DE-AC52-07NA27344.

References

1. E. E. Lewis and W. F. Miller, Jr., *Computational Methods of Neutron Transport*, American Nuclear Society, LaGrange Park, Illinois (1993).

2. J. E. Morel and G. R. Montry, *TTSP*, **13**, 615 (1984).

3. E. W. Larsen and J. B. Keller, *J. Math. Phys.*, **15**, 75 (1974).

4. E.W. Larsen, J. E. Morel, and Warren F. Miller, Jr., *J. Comp. Phys.*, **69**, 283 (1987).

5. K. Thompson, K. Budge, J. Chang, and J. Warsa, Los Alamos National Laboratory Report, LA-UR-05-2256 (2005).

TABLE I

Sums in Eq. (41) for the various angular discretizations in spherical geometry.

Quadrature set order	Sum for MM WDD	Sum for SD	Sum for DD
2	0	7.698004e-01	2.06E-01
4	0.00E+00	4.037247e-01	-3.57E-03
8	-8.33E-17	2.164258e-01	-4.57E-05
10	-4.16E-17	1.755520e-01	-1.21E-05

TABLE II

The sums in Eq. (71) for the angular discretizations in RZ for a Level Symmetric quadrature set.

Quadrature set order	Sum for MM WDD	Sum for DD
2	-4.12E-16	1.42E+00
4	-1.41E-16	1.15E-01
8	1.41E-17	2.09E-02
12	3.39E-16	1.12E-02
16	-1.55E-15	8.82E-03

Figure Captions

Fig. 1. Diagram of the S_2 quadrature set in 1D.

Fig. 2. Coordinate system for R-Z geometry.

Fig. 3. Starting directions, weighted directions, and ξ-levels for a triangular S_6 quadrature set. Starting directions are denoted by "SD".

Fig. 4. Flux dip for Diamond Differencing in spherical geometry for the S_2, ε=1 case.

Fig. 5: Negative flux slope at the origin for Step Differencing in spherical geometry for the S_2, ε=1 case.

Fig. 6. The negative slope at the origin begins to disappear as $\varepsilon \to 0$ for step differencing, S_2, spherical geometry.

Fig. 7. The flux dip disappears as $\varepsilon \to 0$ for diamond differencing, S_2, spherical geometry.

Fig. 8. No flux dip appears for the Morel and Montry weighted diamond angular differencing, S_2, spherical geometry.

Fig. 9. The Morel and Montry weighted diamond angular differencing solution for an S_2 Level Symmetric quadrature set in RZ geometry. Note the lack of a flux dip near the origin for this discretization.

Fig. 10. The flux dip disappears as $\varepsilon \to 0$ for diamond difference in angle S_8, Level Symmetric, RZ geometry.

Fig. 11. Flux dip behavior for the diamond difference discretization in 1D spherical geometry as the quadrature set is refined. This is the ε=1 case.

Fig. 12. Flux dip behavior for the diamond difference discretization in RZ as the quadrature set is refined. This is the ε=1 case with the level symmetric quadrature set.

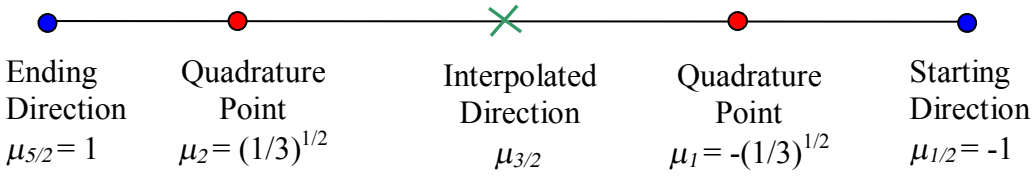

Fig. 1. Diagram of the S_2 quadrature set in 1D.

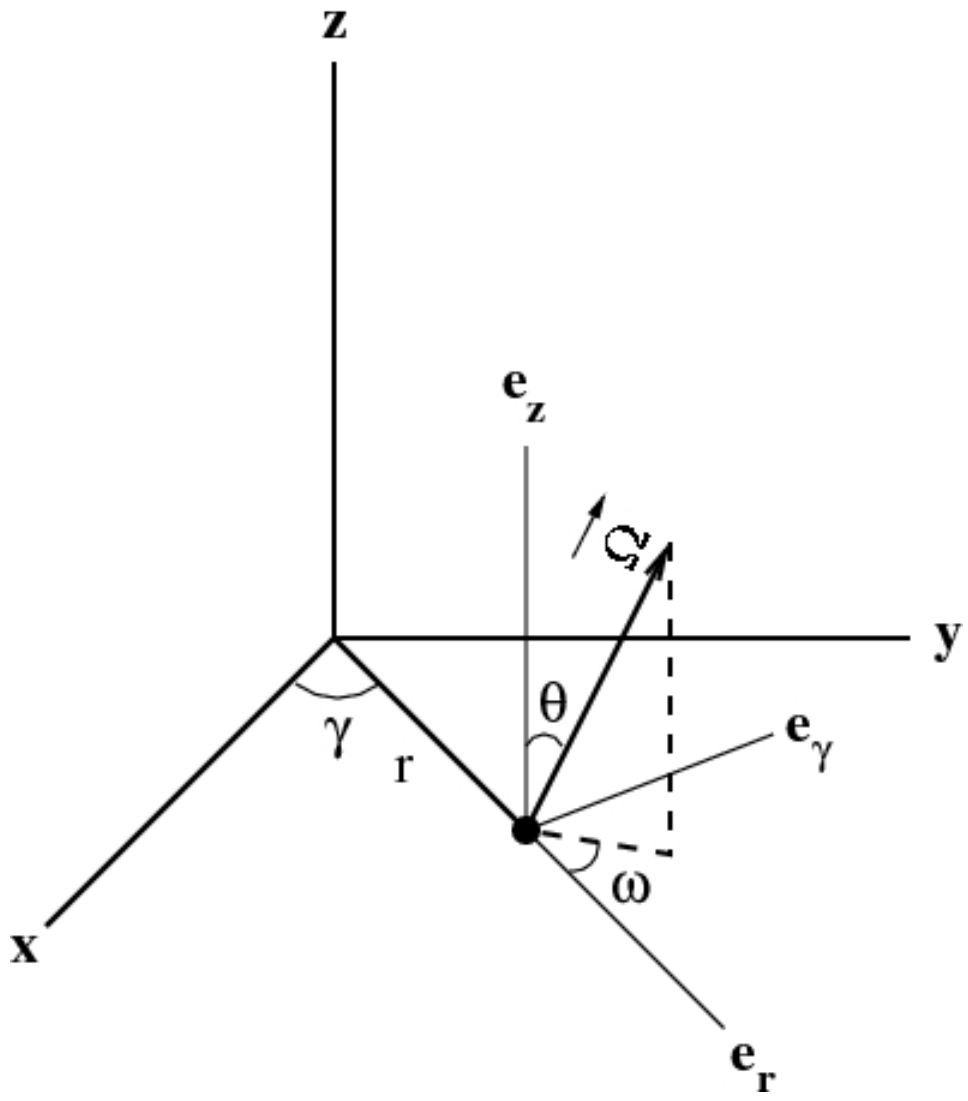

Fig. 2. Coordinate system for R-Z geometry.

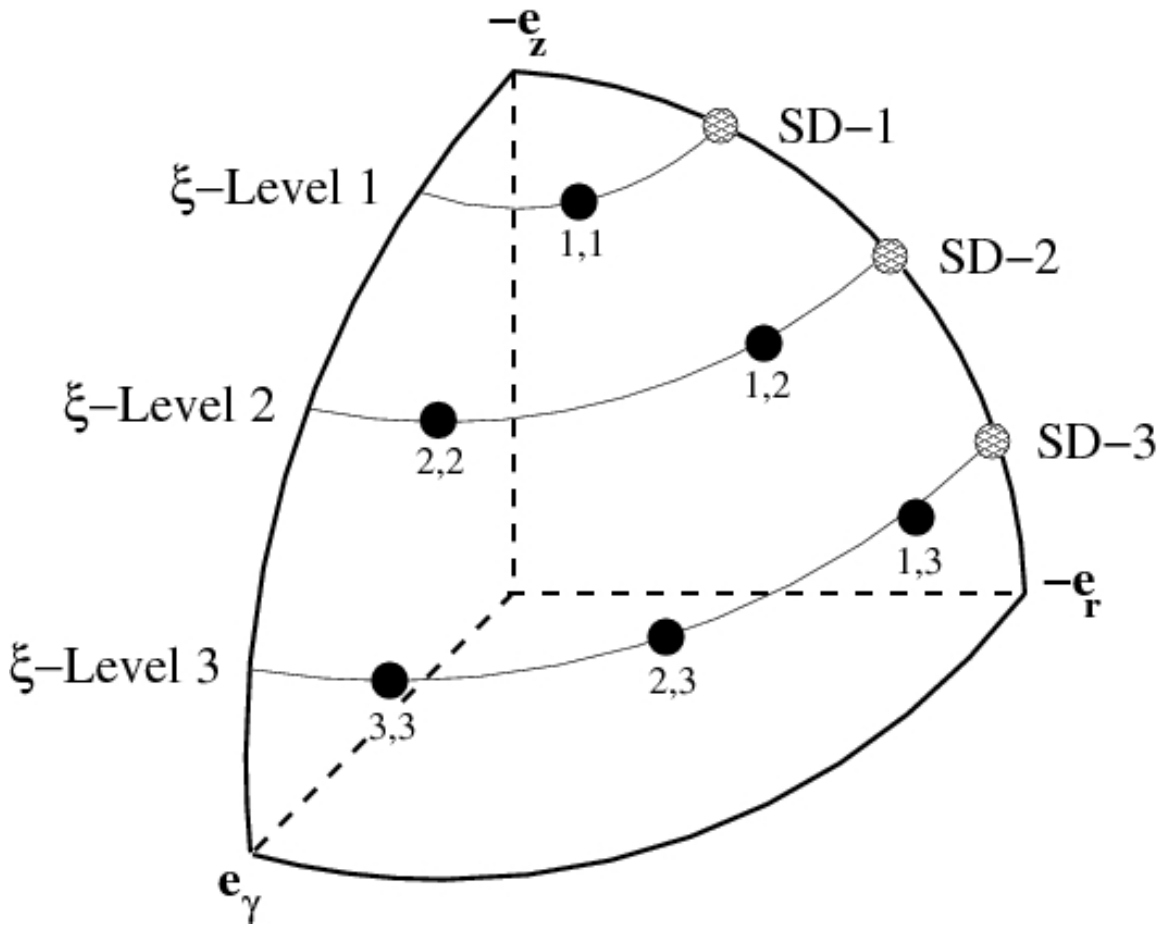

Fig. 3. Starting directions, weighted directions, and ξ-levels for a triangular S_6 quadrature set. Starting directions are denoted by "SD".

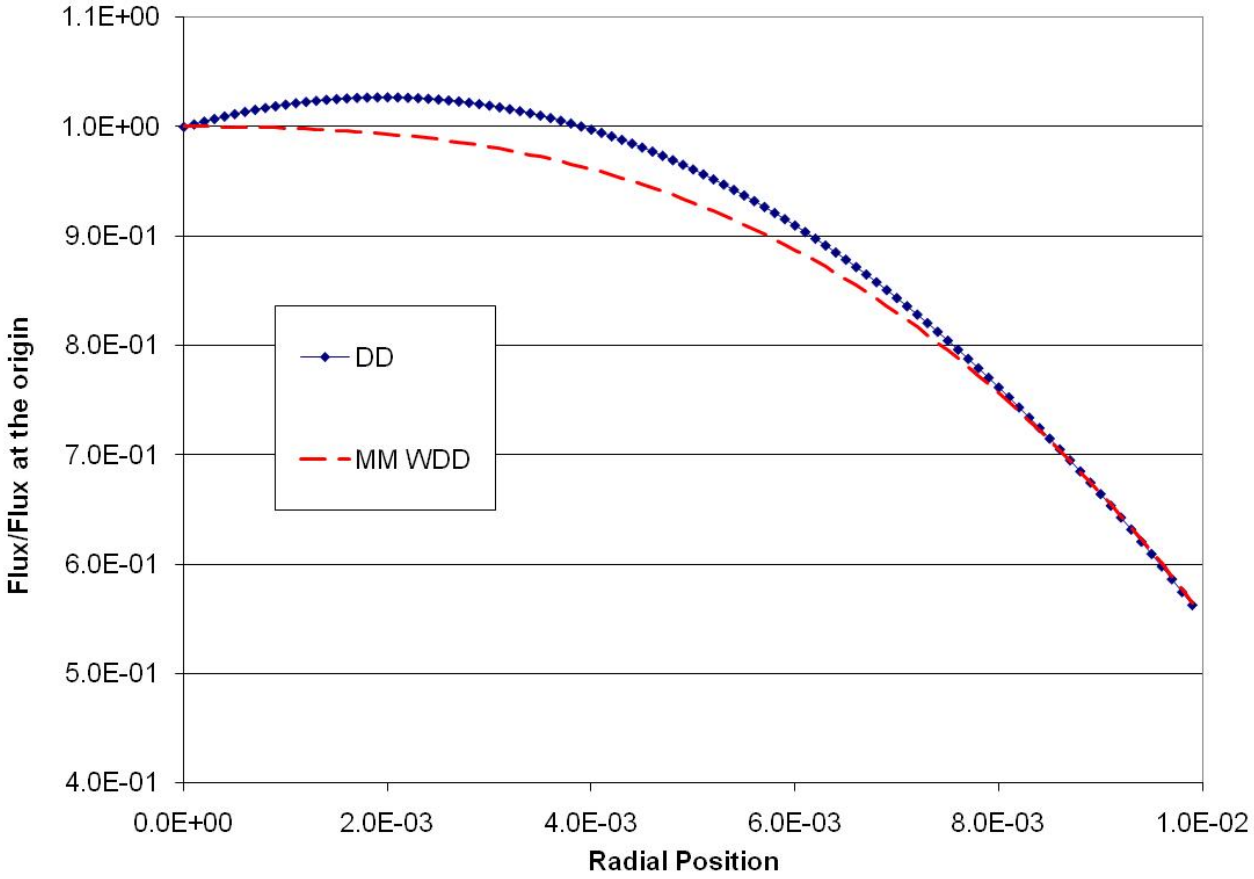

Fig. 4. Flux dip for Diamond Differencing in spherical geometry for the S_2, ε=1 case.

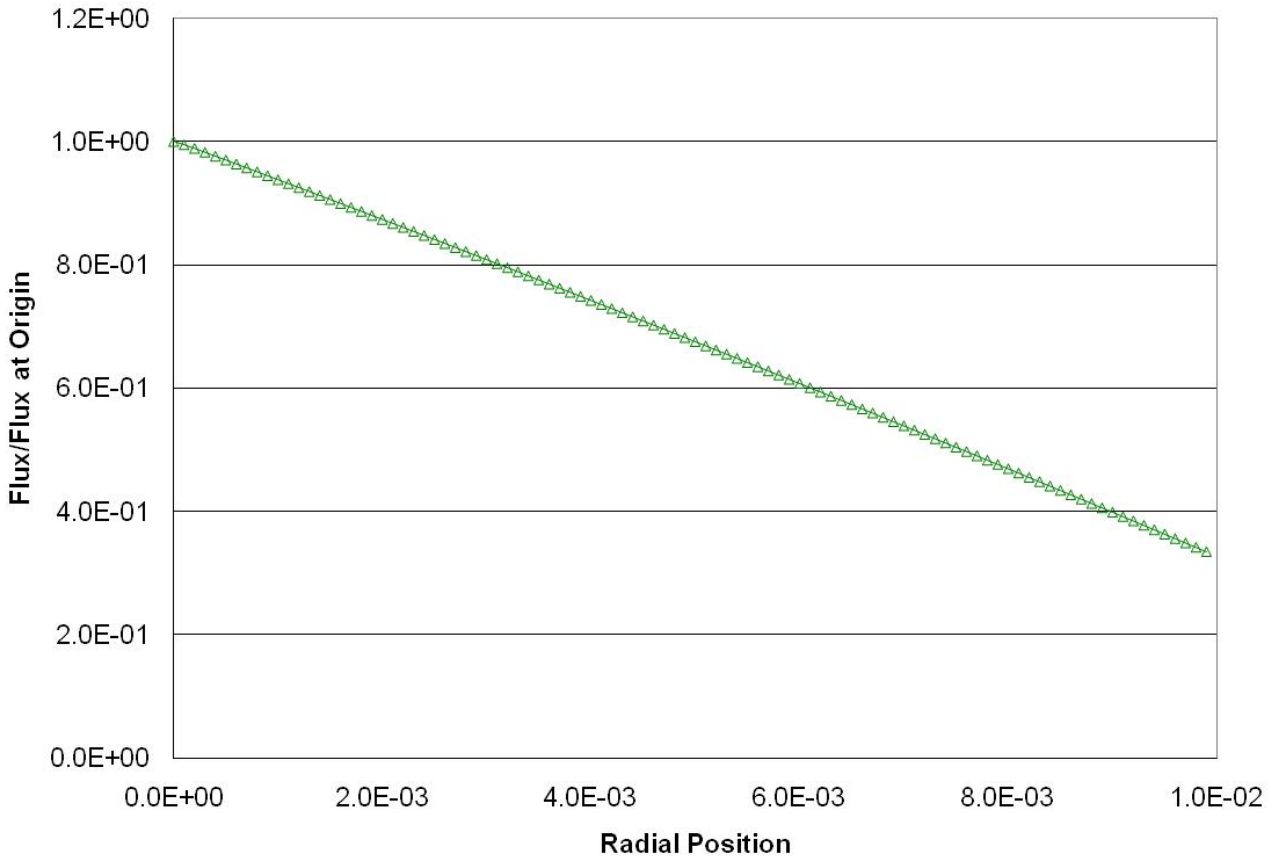

Fig. 5: Negative flux slope at the origin for Step Differencing in spherical geometry for the S_2, ε=1 case.

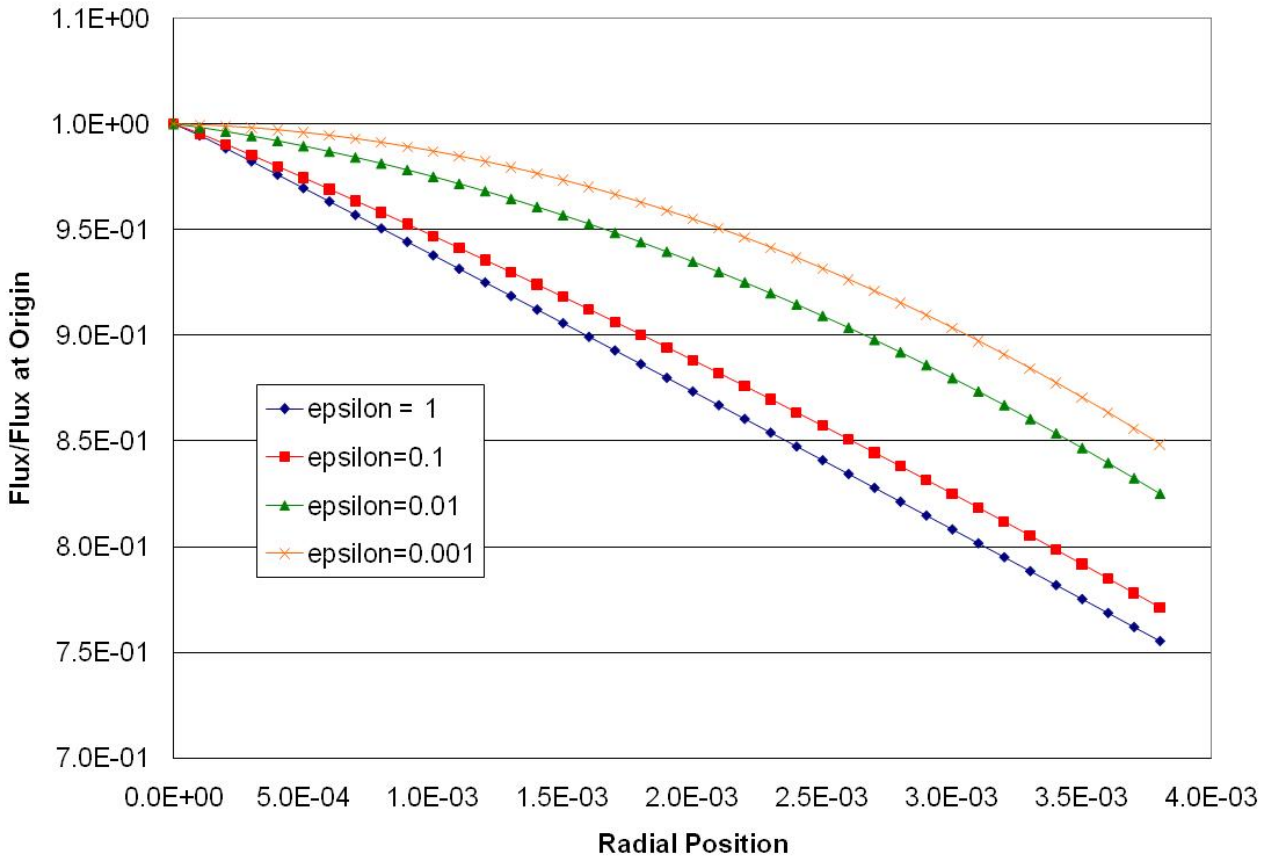

Fig. 6. The negative slope at the origin begins to disappear as $\varepsilon \to 0$ for step differencing, S_2, spherical geometry.

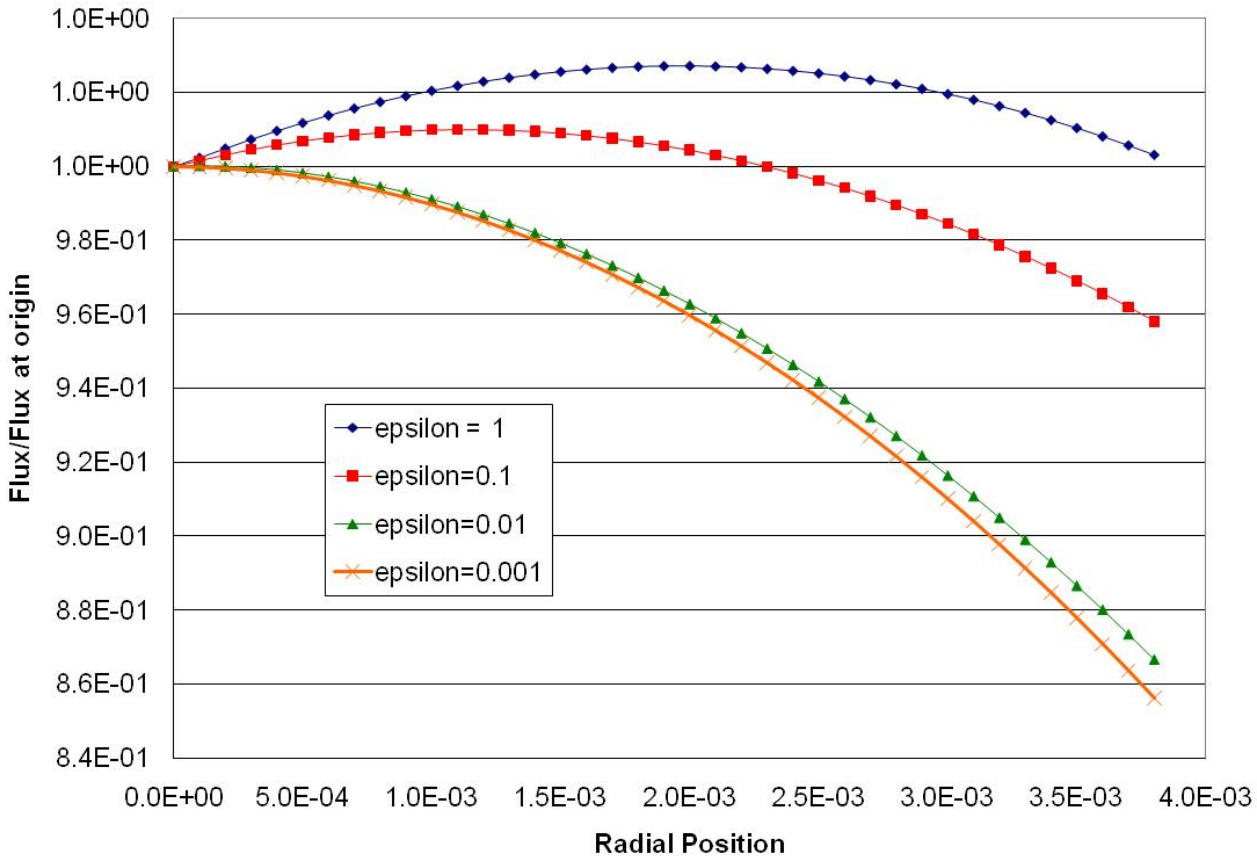

Fig. 7. The flux dip disappears as $\varepsilon \to 0$ for diamond differencing, S_2, spherical geometry.

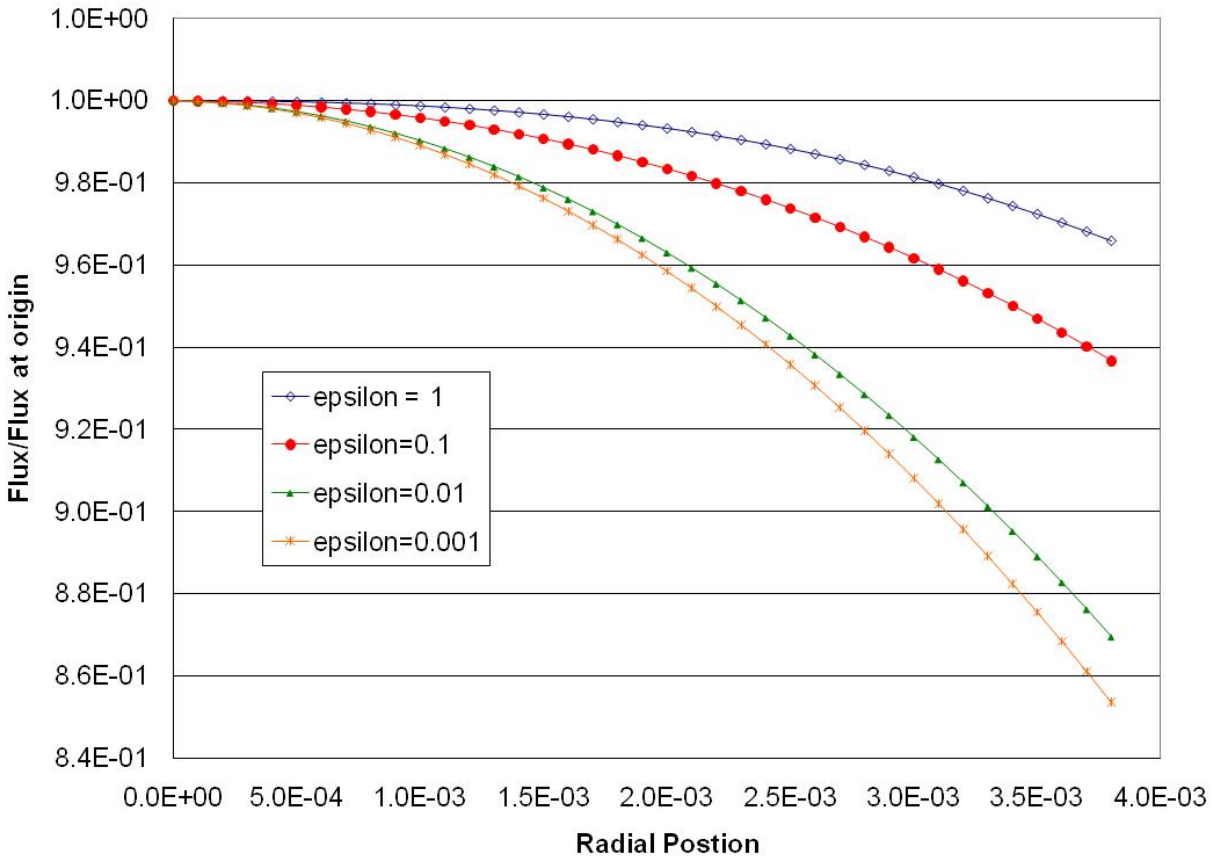

Fig. 8. No flux dip appears for the Morel and Montry weighted diamond angular differencing, S_2, spherical geometry.

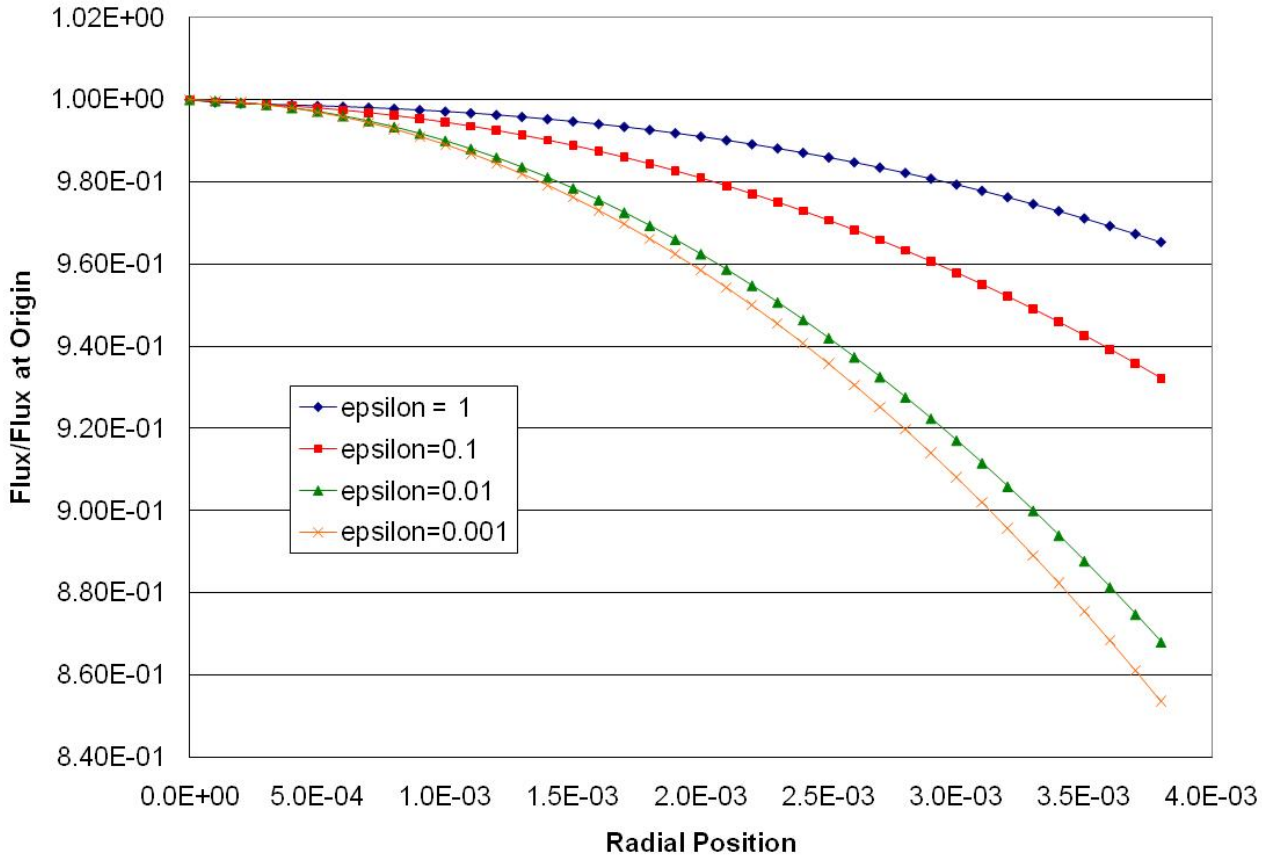

Fig. 9. The Morel and Montry weighted diamond angular differencing solution for an S_2 Level Symmetric quadrature set in RZ geometry. Note the lack of a flux dip near the origin for this discretization.

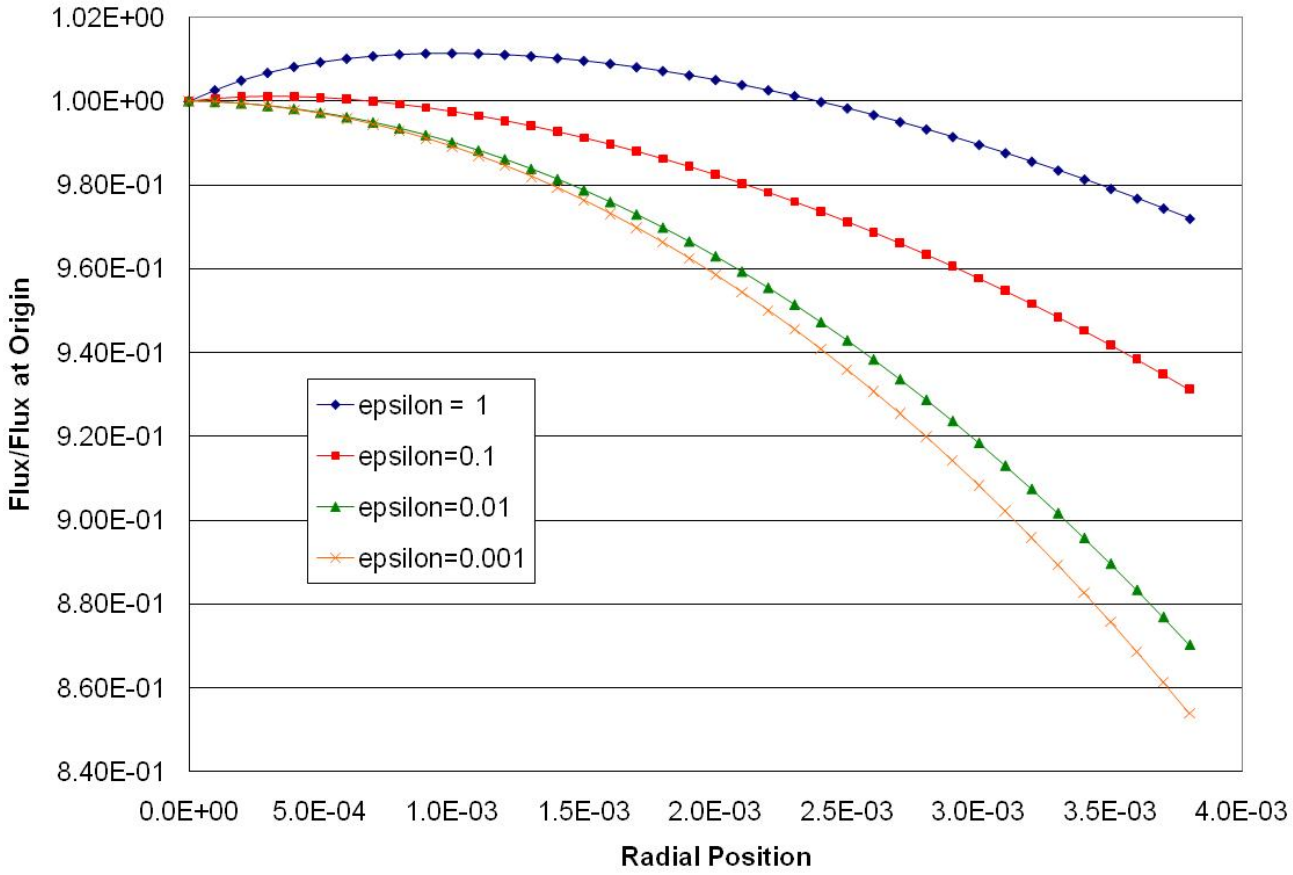

Fig. 10. The flux dip disappears as $\varepsilon \to 0$ for diamond difference in angle S_8, Level Symmetric, RZ geometry.

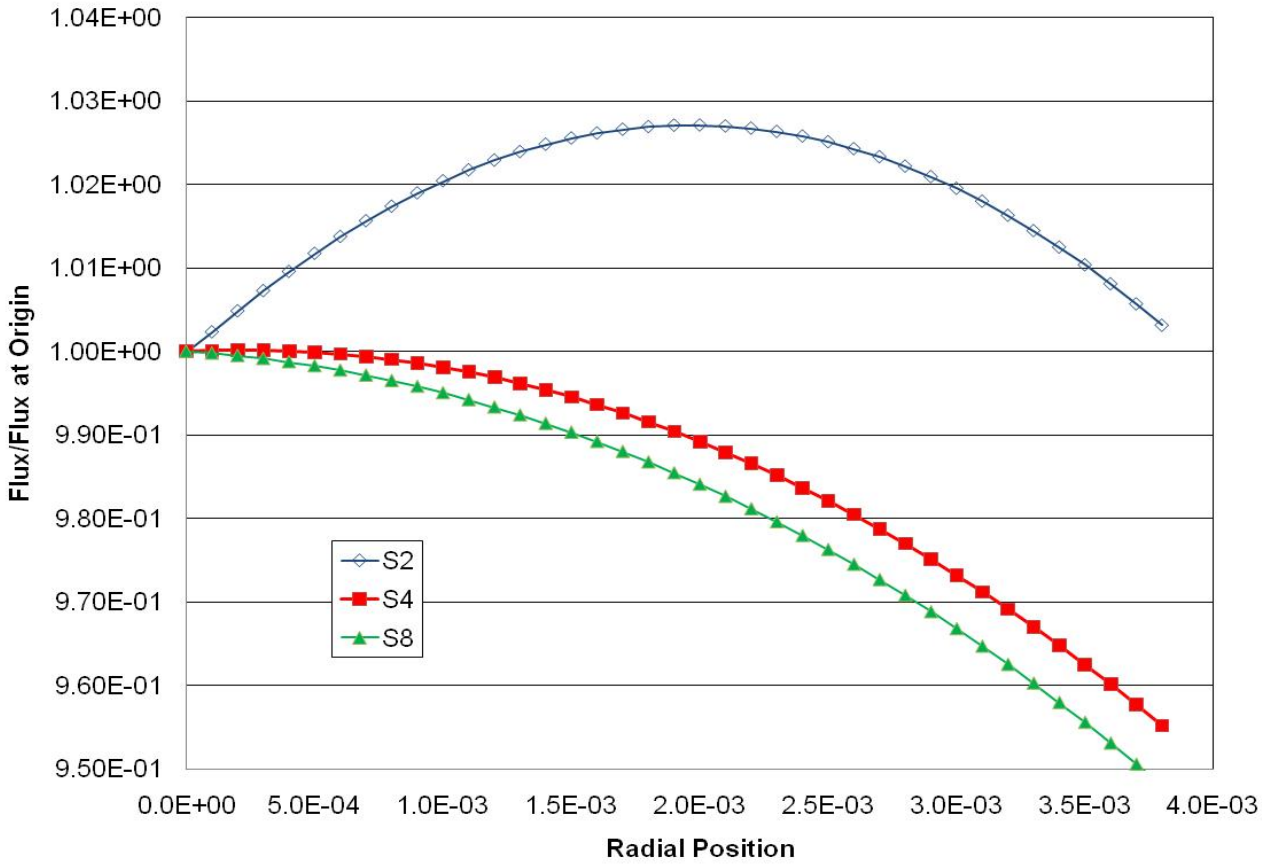

Fig. 11. Flux dip behavior for the diamond difference discretization in 1D spherical geometry as the quadrature set is refined. This is the ε=1 case.

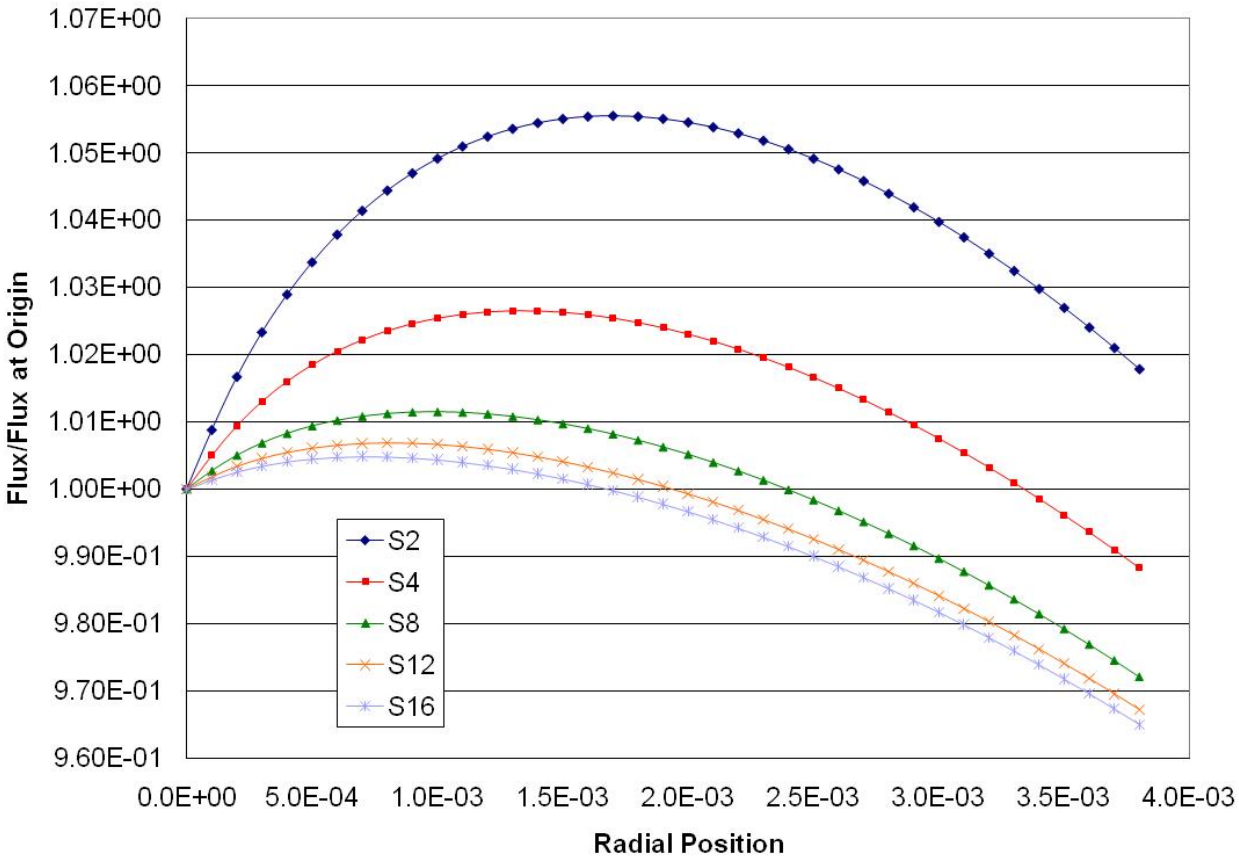

Fig. 12. Flux dip behavior for the diamond difference discretization in RZ as the quadrature set is refined. This is the ε=1 case with the level symmetric quadrature set.